

SPECTROSCOPIC ANALYSIS OF THE DWARF NOVA SS CYGNI

A THESIS

SUBMITTED TO THE GRADUATE SCHOOL

IN PARTIAL FULFILLMENT OF THE REQUIREMENTS

FOR THE DEGREE

MASTERS OF SCIENCE IN PHYSICS

BY

ELIXIA M BENSON-AVILLAN

DR. RONALD KAITCHUCK

BALL STATE UNIVERSITY

MUNCIE, INDIANA

MAY 2010

ABSTRACT

Dwarf novae are a type of cataclysmic variable in which one of the components is a white dwarf. Their outbursts can range in brightness from two to five magnitudes at intervals that can vary from days to decades. The purpose of this study is to analyze the outburst of SS Cygni on the nights of June 18-22, 1987. Using an Interactive Reduction Software (IRS) package and a Gaussian fit program, the emission and absorption line strengths on the rise to outburst showed an increase in the flux as well as various other details supported by theory.

ACKNOWLEDGEMENTS

This project would not have been possible without the support of many people. To my advisor Ronald Kaitchuck, who, with patience, helped me through this process. To my committee members, Mahfuza Khatun and Tomas Robertson, who offered their support throughout my time in the department. Most importantly to my parents, they gave me so much and did everything they could so I could reach my dreams. ¡Gracias!

TABLE OF CONTENTS

ABSTRACT	1
ACKNOWLEDGEMENTS	2
CHAPTER I: DWARF NOVAE.....	6
HISTORY	6
TYPES OF DWARF NOVAE	7
HISTORY OF THE SPECTRAL ANALYSIS OF DWARF NOVAE.....	9
CHAPTER II: ACCRETION DISK	11
CHAPTER III: SS CYGNI.....	15
HISTORY OF SS CYGNI'S DISCOVERY	15
SS CYGNI'S GENERAL INFORMATION.....	15
OBSERVATION OF SS CYGNI AND EQUIPMENT USED	16
CHAPTER IV: DATA ANALYSIS AND RESULTS	20
SUMMARY	45
APPENDIX.....	48
<u>Appendix A: Figure 25: Hertzsprung-Russell diagram.</u> <u>(http://bdaugherty.tripod.com/gcseAstronomy/stars.html).....</u>	48
Appendix B: Example of Output of the Gaussian fit program	49
LITERATURE CITED.....	51

TABLE OF FIGURES

<i>Figure 1: Schematic view of a Cataclysmic Binary. (Warner 1995)</i>	8
<i>Figure 2: Roche Geometry (Caroll & Ostlie 2007)</i>	12
<i>Figure 3: 8.7' x 8.29' image of SS Cygni using the Aladin Sky Atlas</i>	16
<i>Figure 4: Light curve of SS Cygni 1896-1992</i>	17
<i>Figure 5: IDS spectrographs attached to the Perkins 1.8m (72") telescope.</i>	19
<i>Figure 6: Light curve of SS Cygni for the dates of August 23-25, 1985.</i>	23
<i>Figure 7: Light curve of SS Cygni for the dates of September 24-26, 1985.</i>	24
<i>Figure 8: Light curve of outburst for the dates of June 18-22, 1987.</i>	25
<i>Figure 9: Spectrum of SS Cygni for the dates of June 18-22, 1987.</i>	26
<i>Figure 10: Plot of the spectrum on June 19 with the emission and absorption with a Gaussian fit. The fit detected the redshift and blueshift of the accretion disk. The spectrum plotted is from 4750Å to 4950Å</i>	27
<i>Figure 11: Spectrum and Gaussian fit for June 18, 1987.</i>	29
<i>Figure 12: Spectrum and Gaussian fit for June 19, 1987.</i>	30
<i>Figure 13: Spectrum and Gaussian fit for June 20, 1987.</i>	31
<i>Figure 14: Spectrum and Gaussian fit for June 21, 1987.</i>	32
<i>Figure 15: Spectrum and Gaussian fit for June 22, 1987.</i>	33
<i>Figure 16: Flux of the Hβ (4861Å) emission lines vs. Julian date through the outburst.</i>	34
<i>Figure 17: Hβ (4861Å) emission line width vs. Julian date through the outburst.</i>	35
<i>Figure 18: Hβ (4861Å) absorption line Flux vs. Julian date through outburst.</i>	36
<i>Figure 19: Hβ (4861Å) absorption line width vs. Julian date through outburst.</i>	37

<i>Figure 20: HeII (4686Å) emission line flux vs. Julian date through the outburst.....</i>	40
<i>Figure 21: HeII (4686Å) emission line flux vs. Julian date.....</i>	41
<i>Figure 22: Widths of the HeII (4686Å) emission lines vs. Julian date through the outburst</i>	42
<i>Figure 23: Radial velocity of Hβ (λ4861) vs. orbital phase.</i>	43
<i>Figure 24: Radial velocity of HeII (λ4686) vs. orbital phase.....</i>	44
Appendix A: Figure 25: Hertzsprung-Russell diagram. (http://bdaugherty.tripod.com/gcseAstronomy/stars.html).....	48

CHAPTER I: DWARF NOVAE

HISTORY

Cataclysmic stars are stars in which a relatively normal star accretes matter to the smaller companion and their orbits are less than a day long. Dwarf Novae are a type of cataclysmic variable in which the “normal” component is a main sequence star and the smaller component is a white dwarf. The “normal” component, which has its Roche lobe filled, accretes matter onto the white dwarf. This mass flow creates an accretion disk around the white dwarf. The process in which the matter is accreted will be explained on the next chapter.

The discovery of the first dwarf nova was on December 15, 1855 by JR Hind. He recorded the observation of a star that shined as bright as a ninth magnitude star on the 15th and by the 18th was fainter than a 15-magnitude star by half a magnitude or more. Hind was confident that he had found a variable star since he had been observing the region for five years before the discovery. The star was then named U Geminorum and Hind recorded that it had “a very blue planetary light” (Hind, 1856).

By March 26, 1856, Norman Pogson started observing U Gem and confirmed that it was a variable star but that it was not an ordinary nova. Pogson estimated that the

period for the star to reach maximum is around 96 days (Pogson, 1857). This led to a series of observations by other astronomers like Knott, Baxendell, Turner, among others.

In 1896 another member of this class of variable was discovered, SS Cygni. The discovery was made by Louisa D. Wells as described by Pickering (1896). In 1865, Peters (1865) believed to have discovered a nova, T Leonis, but it was later found to be a dwarf nova. By 1904, Z Camelopardalis had been discovered and had become the prototype of the third subclass of dwarf nova (van Biesbroek, 1904).

By the 1960s, the initial suspicion that dwarf novae are binaries was confirmed thanks to spectroscopic studies that revealed periodically changing radial velocities in these systems. In the 70s and 80s the development of red sensitive CCDs (Charge Coupled Devices) allowed the studies to extend their range from the optical part of the spectrum to the near infrared allowing the observers to detect an increasing number of faint red secondary components. With the creation of ultraviolet satellites, like the Hubble Space Telescope, white dwarfs were easily detected. (Connon Smith, 2007)

TYPES OF DWARF NOVAE

Dwarf novae have outbursts that can range in brightness from two to five magnitudes at intervals that can vary from days to decades. They are divided by the characteristics of their light changes into three subclasses: UGSS (SS Cygni-type variables), UGSU (SU Ursae Majoris-type variables) and UGZ (Z Camelopardalis-type variables).

UGSS variables increase in brightness by 2-6 magnitudes in V in 1-2 days and return to their original brightness in the following days. Their cycles can last from 10 to

thousands of days. UGSU variables have two types of outbursts: a “normal” and a “super outburst”. The “normal” are similar to the outbursts of the UGSS outbursts while the “super outburst” are brighter by two magnitudes, last more than five times longer than the “normal” and are less frequent. During “super outburst”, the light curve shows superposed periodic oscillations in which their period is close to the orbital period with amplitudes about 0.2-0.3 magnitude in the V. Their orbits are shorter than 0.1 days and the companions are of spectral type dM. UGZ variables also show cyclic outbursts, they sometimes do not return to the original brightness but during several cycles retain a magnitude between maximum and minimum. Their cycles can range from 10 to 40 days and the light amplitudes from magnitude 2 to 5 in V (Samus, 2004).

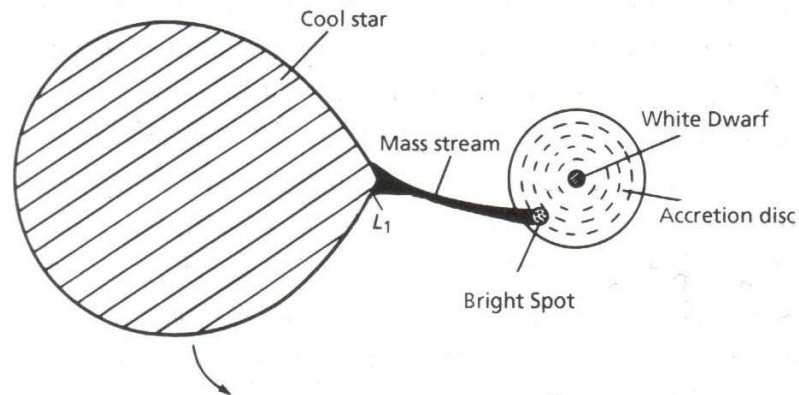


Figure 1: Schematic view of a Cataclysmic Binary. (Warner 1995)

U Gem and SS Cyg belong to the UGSS subclass, T Leo belongs to the UGSU subclass and Z Cam belongs to the UGZ subclass. Each subclass' name is obtained from the variable that best describes the subclass. For UGSS, even though U Gem is mentioned as one of the precursors, is named after SS Cygni. For UGSU is SU Ursae Majoris, and for UGZ is Z Camelopardalis.

HISTORY OF THE SPECTRAL ANALYSIS OF DWARF NOVAE

Copeland (1882) and Knott (1882) made the first spectrum observation of a dwarf nova with their observation of U Gem. The earliest observations of U Gem and SS Cyg at maximum light occurred during the Henry Draper objective prism survey (Fleming 1912). A series of scientists began studying the variations between the minimum spectrum and the maximum spectrum (Adams et al. 1921, Wachmann 1935, Joy 1940, Elvey et al. 1943, Hinderer 1949). They noted that at maximum, the flux distribution matches that of A1-A2 stars and at minimum emission lines of H, HeI, HeII ($\lambda 4686$) and CaII were detected as well as the Balmer continuum in emission.

In 1940, Joy discovered that the dwarf nova RU Peg had a dG3 absorption spectrum and an emission-line spectrum. dG type white dwarfs are now in the dZ type classification, which has metal emission lines and no H or He lines present. Joy later found that SS Cyg had a combined spectrum from which, using the radial velocity variations, he was able to find the orbital period of 6h and 58min (Joy 1956). In 1954 Walker discovered that DQ Her was an eclipsing binary and this discovery, along with the previous ones, helped Kraft (1962) speculate that all the cataclysmic variable stars are binary systems.

Crawford and Kraft (1956) did a detailed study of AE Aqr and discovered that the secondary fills its Roche lobe. They deduced that the broad emission lines were from turbulent gas passing from the secondary star spinning around the white dwarf primary. Smak (1969) did calculations of the line profiles of the double emission lines in many cataclysmic variables showing evidence of a disk.

Kraft also did an extensive survey of the spectra of the cataclysmic variables and discovered that the orbital motion could be measured in almost all of them and that the cataclysmic binaries are close binaries in which the companion transfers mass to the white dwarf (Kraft 1964).

CHAPTER II: ACCRETION DISK

The formation of the accretion disk is possible when one of the stars in a binary system fills the Roche Lobe. The Roche Lobe is the region surrounding each star in which the material is gravitationally bound. There are five points in which a small object, only affected by gravity, appears stationary since the forces cancel out; they are known as the Lagrangian points. As the main sequence star expands, it fills its Roche lobe allowing gas to flow through the inner Lagrangian point L_1 and with the momentum of the star's orbital motion create an accretion disk around the white dwarf. The mass accreted will not collide with the star but it will orbit around the primary creating an accretion disk larger than the radius of the primary star and smaller than the separation of the stars.

Figure 2 shows the equipotentials and effective potential of a system in the rotating frame in which $M_1 = 0.85M_\odot$, $M_2 = 0.17M_\odot$ and the distance between the stars is $a = 5 \times 10^8 m = 0.85R_\odot$. As observed L_1 has a lower potential than the Lagrangian points 2 and 3, therefore as M_1 fills the Roche lobe with matter the matter flows towards M_2 the accretion disk is formed.

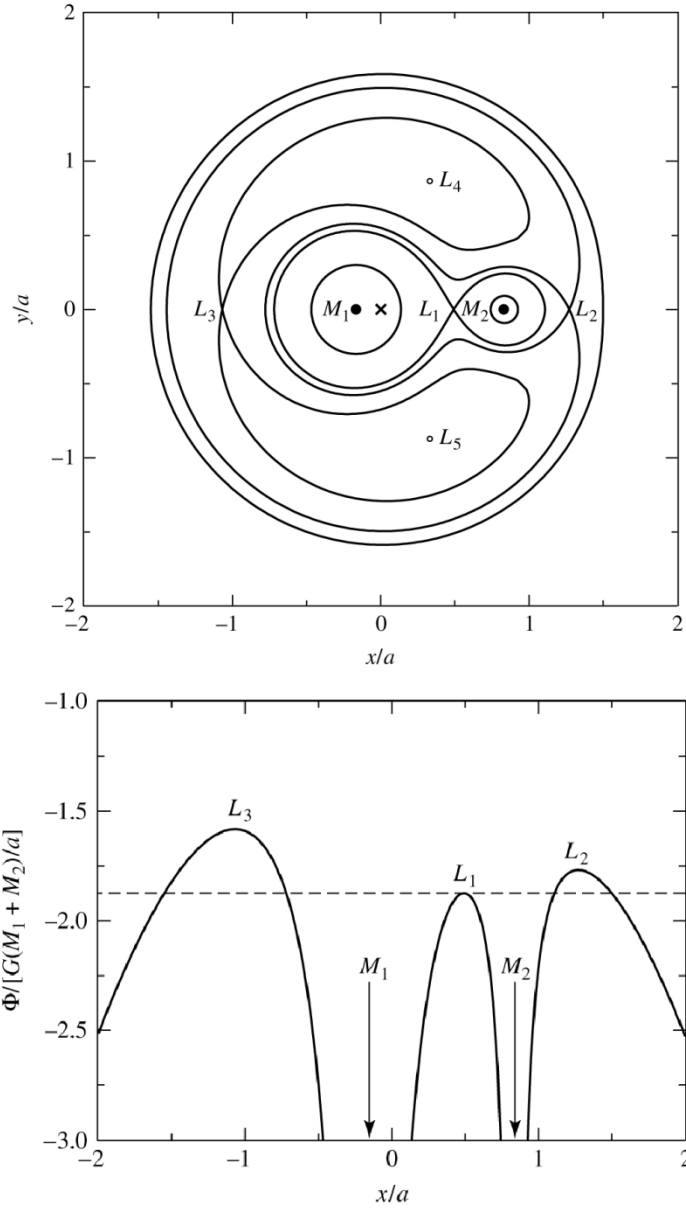


Figure 2: Roche Geometry (Caroll & Ostlie 2007)

There are two main theories of what causes an outburst. The first theory explains that the outburst occurs when material from the secondary star is accumulated in the outer ring of the accretion disk and then is suddenly accreted into the white dwarf (Smak,

1984). The second theory assumes that the outburst occurs due to the sudden increase in the mass transfer to the white dwarf (Paczynski 1971).

The thickness of the disk is established by the hydrostatic equilibrium, which implies a thin disk structure. Since the majority of the disk is so close to the white dwarf the gravitational field of the secondary star can be ignored. There are different ways in which the accretion disk can be detected: the contribution from the disk to the total light of the system, obscuration of the primary star by the disk, occultation of the disk by the secondary star and occultation of the secondary star by the disk. Most of the contribution from the disk is detected in the form of emission lines. Due to the rotational velocity of the disk double emission lines can be detected. In addition, whenever the disk is occulted there are major variations on the profile of the emission lines (Smak 1989).

The standard accretion disk theory assumes that the disk is axially symmetric, flat and follows a Keplerian behavior. The disk contributes significantly to the system total light in case the mass transfer is high and the primary has a low mass since the luminosity depends on the mass of the primary star.

If the outburst occurs when material from the secondary star accumulates in the outer ring of the accretion disk and then is suddenly accreted onto the white dwarf, the disk becomes unstable as the material accumulates in the disk. Once completely unstable the outburst is observed; this instability is a thermal instability. As the outburst begins, the temperature increases generating different emission lines in the process. After the outburst, the disk becomes stable. Because the accreted mass continues to flow the instability is once again formed and the outburst is once again created. This instability can last from 2 to 10 weeks, or even longer.

The outburst could also be a result of a sudden increase in the matter transfer to the white dwarf. This can be caused by instability in the atmosphere of the secondary star, which may cause the disk to collapse. As the disk collapses, the matter is dumped into the white dwarf increasing the brightness of the system.

Of both theories, the instability model is favored. This is so mainly because it offers a definite mechanism for the cause of the outburst and the simulations with this model have successfully explained many of the characteristics of the dwarf novae outburst. (Warner, 1995)

CHAPTER III: SS CYGNI

HISTORY OF SS CYGNI'S DISCOVERY

Louisa D. Wells of the Harvard College Observatory first discovered SS Cygni's variability in 1896. The details of the discovery have not been found but the plates at the Harvard Observatory date the discovery before September 23, 1896. The discovery was announced at the Harvard College Observatory Circular on November 12, 1896. In it the author indicated that the period appeared to be of about 40 days, the brightness varied from 7.2 to fainter than 11.2 and that this was "an unusually large range for a variable having such a short period" (Pickering, 1896).

SS Cygni has been observed continuously ever since it was discovered in 1896. This can be seen in Figure 4 in which the observations from 1896 to 1992.

SS CYGNI'S GENERAL INFORMATION

SS Cygni is located at RA: 21h 42m 42.804s DEC: +43° 35' 9.88" (FK5 J2000). Figure 3 shows a 8.7' by 8.29' image of SS Cygni in the sky. It has a magnitude at minimum brightness of 12.4 and at maximum brightness of 7.7. The outbursts are observed in a quasi periodicity of 49 days; the orbital period is of 6.6013 hours and the binary is composed by a K5V, an orange dwarf (similar to 61 Cygni A which can be

observed in appendix A in the HR diagram), and a white dwarf. At quiescence, it has a mass transfer rate of approximately $6.66 \times 10^{-9} M_{\odot}/\text{year}$ (Patterson 1984, Warner 1987a).

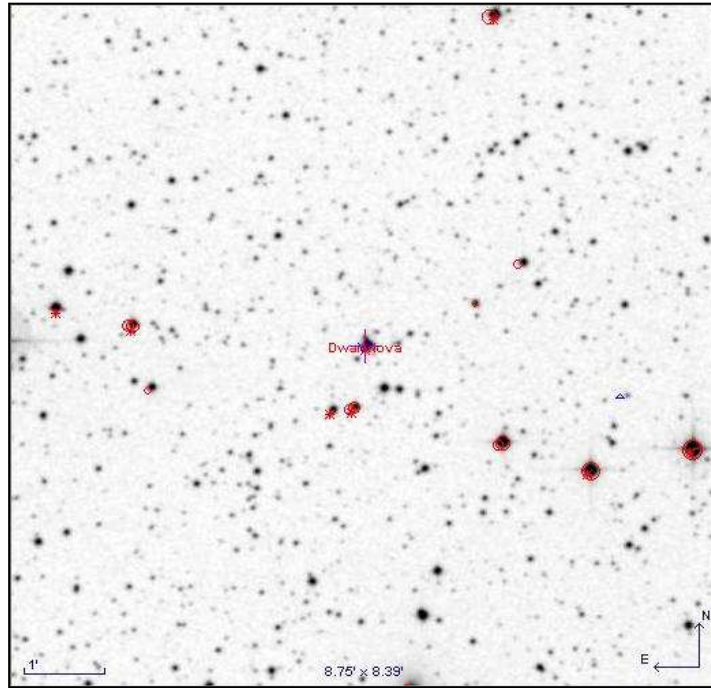


Figure 3: $8.7' \times 8.29'$ image of SS Cygni using the Aladin Sky Atlas (Bonnarel et al., 2000)

OBSERVATION OF SS CYGNI AND EQUIPMENT USED

During the dates of August 23-25, 1985, September 24-26, 1985 and June 18-22, 1987 Ronald Kaitchuck obtained a series of spectra. These consisted of standard stars, the FeNe comparison lamp, flat fields and spectra from SS Cygni. During the dates of June, SS Cyg was observed at mid-outburst while the August and September dates were between the outbursts. The data covers the spectrum from 4270\AA to 5090\AA with a center

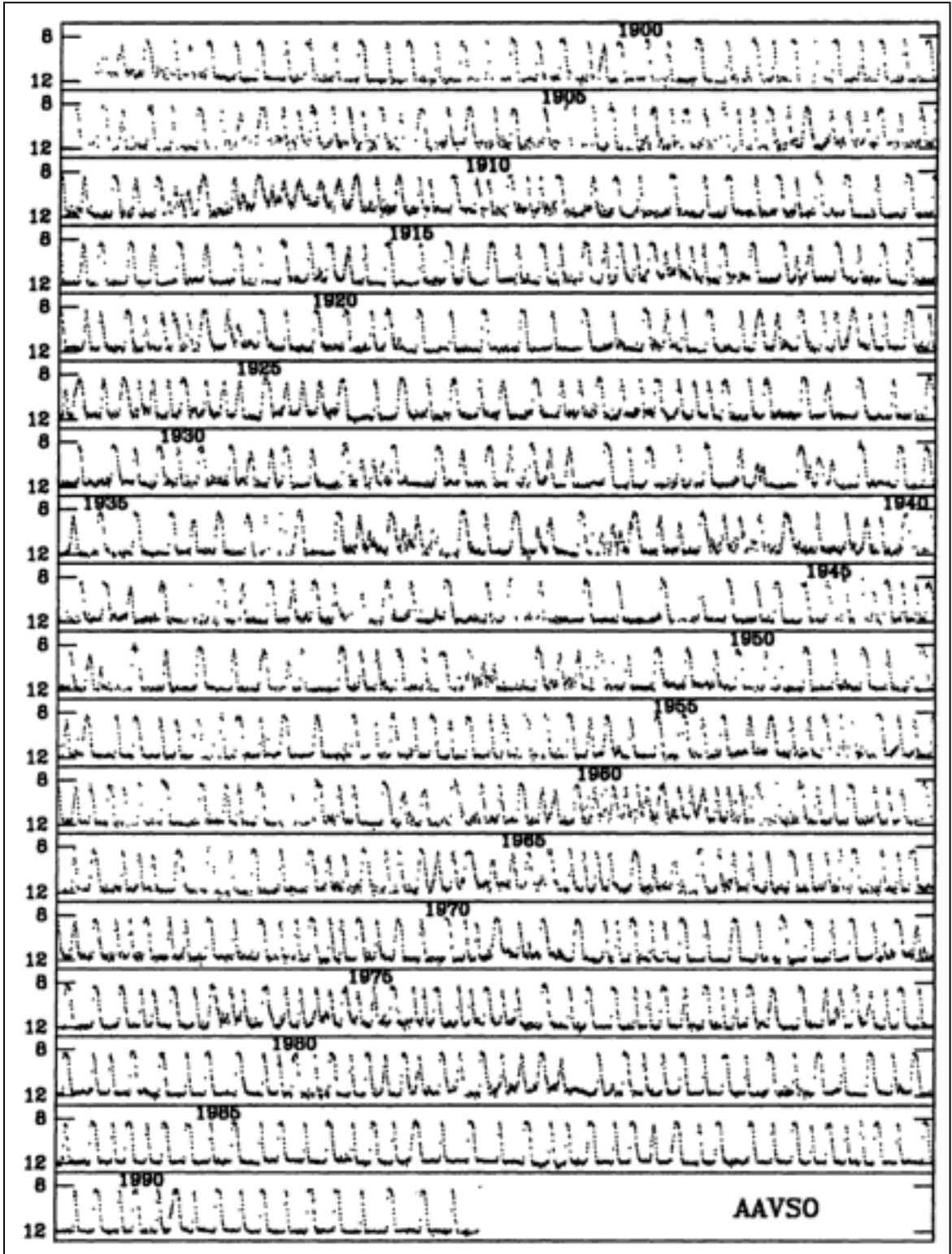


Figure 4: Light curve of SS Cygni 1896-1992

wavelength of 4680\AA , this was an excellent choice since the $H\beta$ ($\lambda 4861$), $HeII$ ($\lambda 4686$) and $H\gamma$ spectral lines can be observed in that range.

The telescope used was the 1.8m Perkins telescope located on Anderson Mesa in Flagstaff, Arizona. The telescope has a Cassegrain optical system and a German equatorial mounting (Figure 5). At first belonging to a partnership between the Ohio Wesleyan University and Ohio State University it is now part of a partnership between the Lowell Observatory and Boston University and it is located at an altitude of 7236 ft (2206m) and it has a focal ratio of 17.5.

The spectrograph used was the Image-Dissector Scanner (IDS). It has two round entrance apertures that have an area of 3 arc sec squared and are separated on the sky by 36 arc sec. The radiation that passes through the apertures is collimated by an inverted Cassegrain collimator with an f-ratio that matches the f-ratio of the Perkins telescope. This spectrograph had attached a Schmidt Cassegrain semisolid camera with a focal length of 140 mm. The acquisition camera has a usable field of $\sim 30 \times 20$ arc min, large enough for field recognition and small enough for accurate centering of the desired object. The system has a limiting magnitude of ~ 12 . (Byard et al., 1981)



Figure 5: IDS spectrographs attached to the Perkins 1.8m (72") telescope.

CHAPTER IV: DATA ANALYSIS AND RESULTS

As previously stated this study uses the data obtained by Ronald Kaitchuck during the dates of August 23-25, 1985, September 24-26, 1985 and June 18-22, 1987. The focus of the study is on the June data since the system was in outburst at that moment. The datum is a spectrum that covers from 4270Å to 5137Å. In this range, the lines H β (λ 4861), HeII (λ 4686) and H γ (λ 4340) can be detected. Unfortunately, the H γ (λ 4340) spectral line could not be analyzed since there was too much noise in the region of the line.

As a first step, the data are compared to the data from the American Association of Variable Star Observers (AAVSO). AAVSO has collected the light curves of many variable stars throughout the years thanks to the contribution made by many observers. In their website, the visitor can obtain the light curve of the desired dates and the values for each point. Figures 6 through 8 show a comparison between the data used in this study and the data from AAVSO.

How is it possible to do photometry with a spectrograph? Slit based spectrographs have a fixed resolution but starlight that doesn't pass through the slit is lost. The apertures of the spectrograph used in this study are round therefore there is a

bigger area to accept the entire star image. This allows the spectrograph to measure the flux from the system but it has a lower resolution.

There are some similarities in the values of the data but will not be the same because the AAVSO data are visual observations and the data used here is in the blue portion of the electromagnetic spectrum. The August data (Figure 6) shows a constant magnitude throughout the nights and the September data (Figure 7) shows a decrease of the magnitude of the system. When trying to explain why did this occur no real explanation was found. The first night, as observation began, the sky was in twilight most likely changing the sky transparency. Another thing that could be what affected the datum is the weather, the day before the observation started there was rain and thunderstorms and on the first day there were some scattered clouds. The June data (Figure 8) are very similar to the AAVSO data. There is more June data since the main purpose when observing dwarf novae has been to explain the behavior of the systems during outburst.

To process the data the Interactive Reduction Software (IRS) was used (Peterson 1988). The IRS would plot and identify the spectra of SS Cygni as well as display information regarding the place of observation, the observer and any notes made by the observer. With the IRS an average of the spectra of each night was made. The resulting average was then plotted and compared to the rest of the nights (Figure 9). As the nights went by it can be seen that the H β (λ 4861) emission lines at first decrease in flux to later increase as well as an increase in the absorption line strength. There is, as well, an increase in the HeII (λ 4686) emission line. For the June 22 data any reason for why the data's quality was poorer than the previous night could not be obtained.

When trying to understand why the June 22 data was poorer than the previous night there were no records in the notes of the weather or if anything else could affect the data even the Weather Underground website showed that that day and the day after the sky was clear. Figure 9 shows the decrease of the H β (λ 4861) emission line and an increase in the H β (λ 4861) absorption lines throughout the outburst. It is also noticeable the increase of the HeII (λ 4686) emission lines from mid outburst.

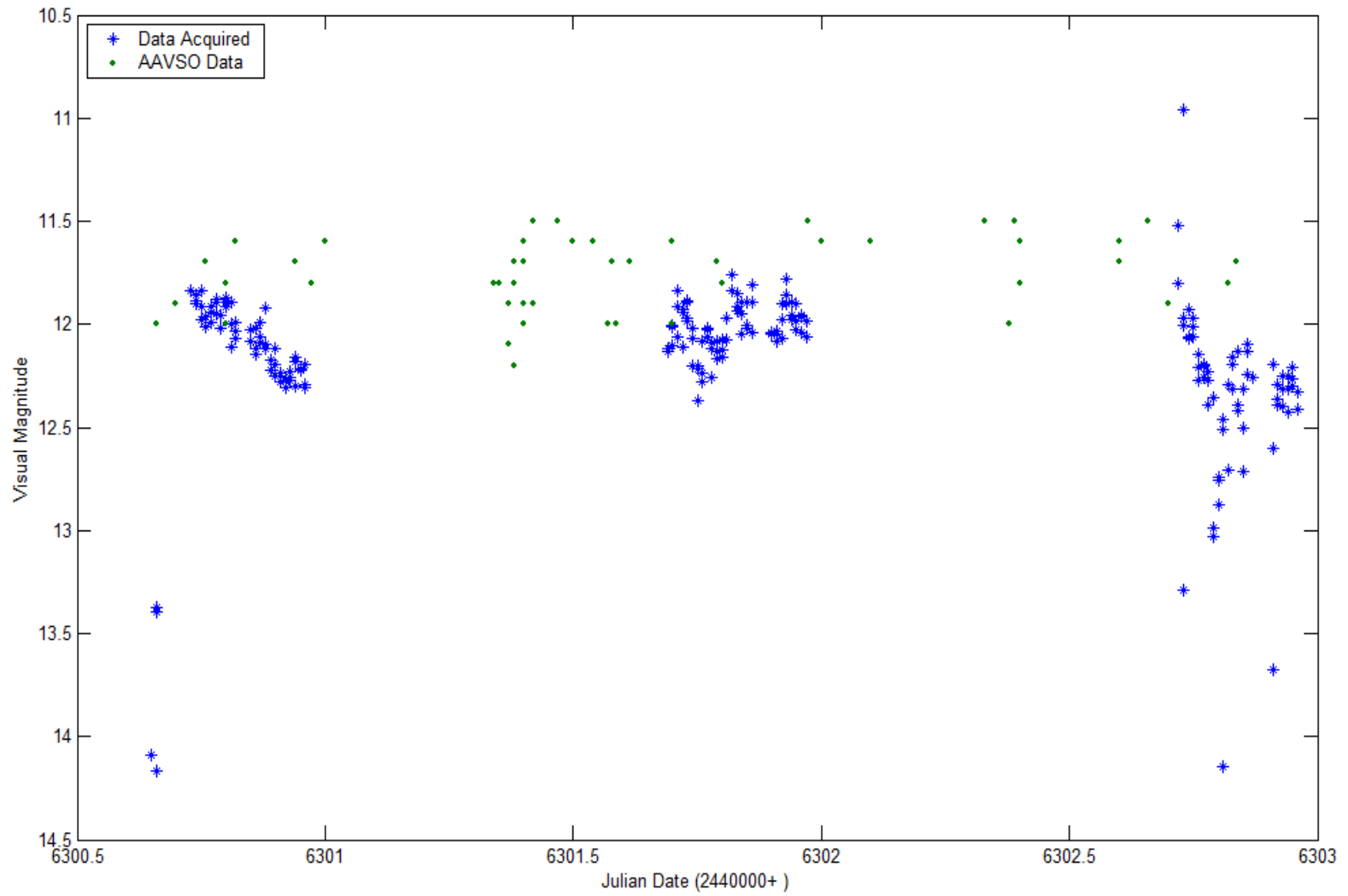


Figure 6: Light curve of SS Cygni for the dates of August 23-25, 1985.

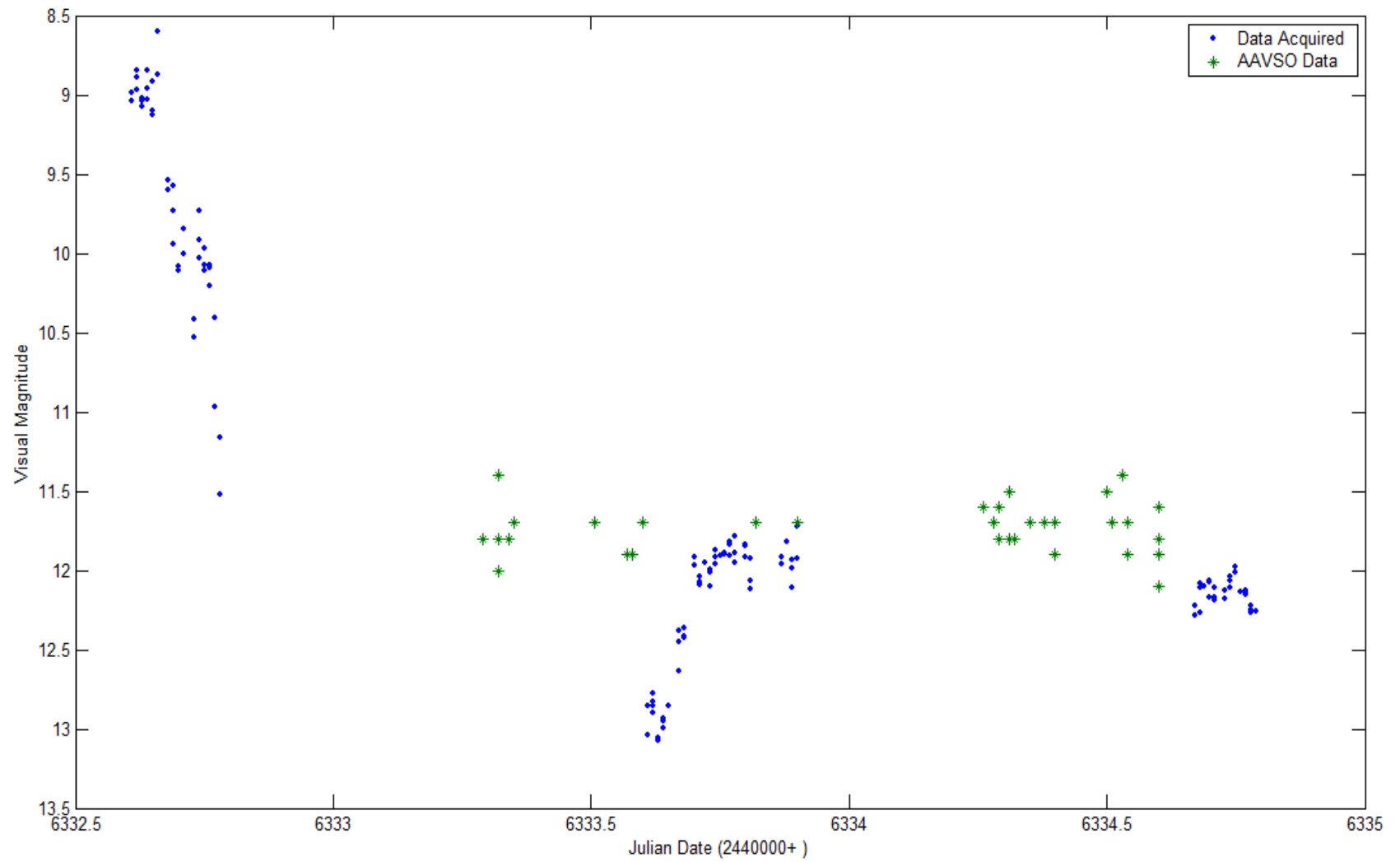


Figure 7: Light curve of SS Cygni for the dates of September 24-26, 1985.

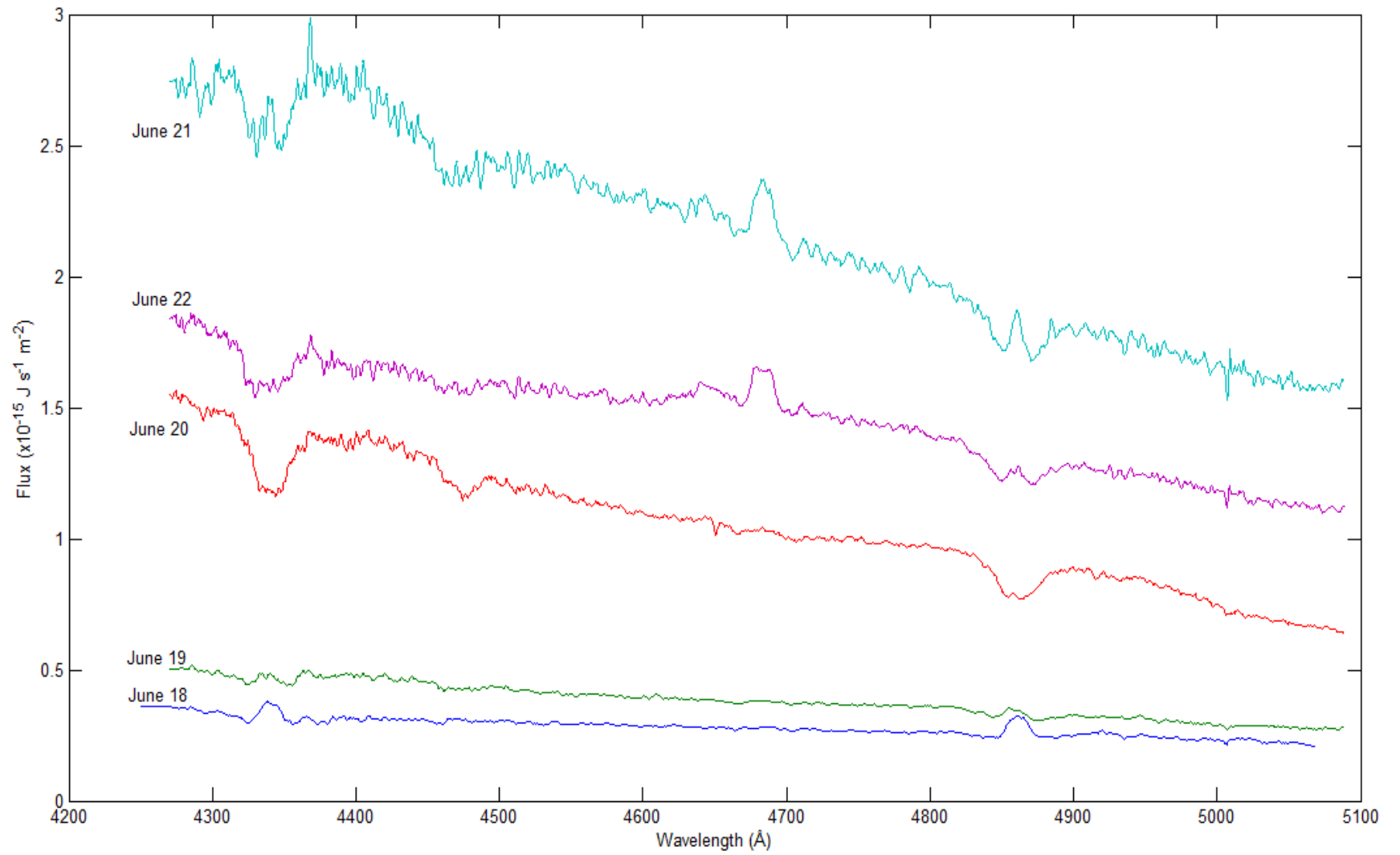


Figure 9: Spectrum of SS Cygni for the dates of June 18-22, 1987.

The next step was to use a Gaussian fit program on the all the spectra including the average data of each night. H β (λ 4861) emission and absorption lines were fitted for the nights of the 18th through the 20th while, for the nights of the 21st and the 22nd, H β (λ 4861) absorption and HeII (λ 4686) emission lines were fitted. On the data of June 19 some spectra showed a double peak in H β (λ 4861) therefore a fit for the double peaks was made. Remember that these lines come from the accretion disk, therefore if there is presence of double emission lines it is because the photons come from different parts of the accretion disk. Figure 10 is a screen shot of the IRS software comparing the one of the files of June 19 and the Gaussian fit. It shows how well the Gaussian fit worked fitting the two emission lines and the absorption line in H β (λ 4861).

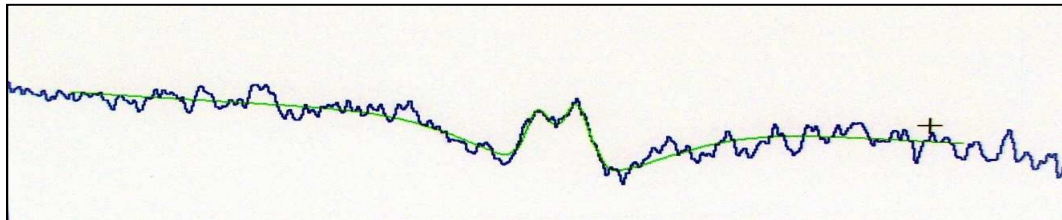


Figure 10: Plot of the spectrum on June 19 with the emission and absorption with a Gaussian fit. The fit detected the redshift and blueshift of the accretion disk. The spectrum plotted is from 4750Å to 4950Å

The Gaussian fit output had information regarding each file, some were regarding the way the program works and others were about the spectra. To ensure that the results were correct some information in the output had to be verified. A value that needed to be verified was the integrated line flux. This flux was compared to the integrated flux error given by the FIDO sub-routine. As long as the flux was much bigger than the error, the resulting fit would be accepted. This is so because if the flux and the error were close in

values then the program would not have obtained a proper fit of the file. An example of the output can be observed in Appendix B.

Once all the values were verified, the analysis of the other values found on the data could be done. As previously mentioned an average of the spectra of each night was done. These resulting spectra were then fitted to H β (λ 4861) emission lines, H β (λ 4861) absorption lines or HeII (λ 4686). Using mathematical graphing software, the spectra and the fits were plotted and can be seen in figures 11 through 15. For the June 22 plot (Figure 15), the H β (λ 4861) emission line detected could not be fitted which shows that the emission and the absorption at this stage come from two different regions.

On the data obtained on June 19 double peak in the H β (λ 4861) emission lines in some files was detected. Figure 16 shows the behavior of the H β (λ 4861) emission line flux throughout the outburst. On the first night, it is seen how the flux is scattered and it clumps by the next night then by the 4th night the flux is scattered. Figure 17 shows a decrease in the overall data of the width of the H β (λ 4861) emission lines. Figure 18 shows how the H β (λ 4861) absorption flux lines have the same behavior as the magnitude of the system throughout the outburst. Meanwhile, figure 19 shows how the datum is scattered on the first days of the observation dates and on the last days of observation while on the third day the datum is cluttered and has a lower average than the other nights and it is consistent with the error bars.

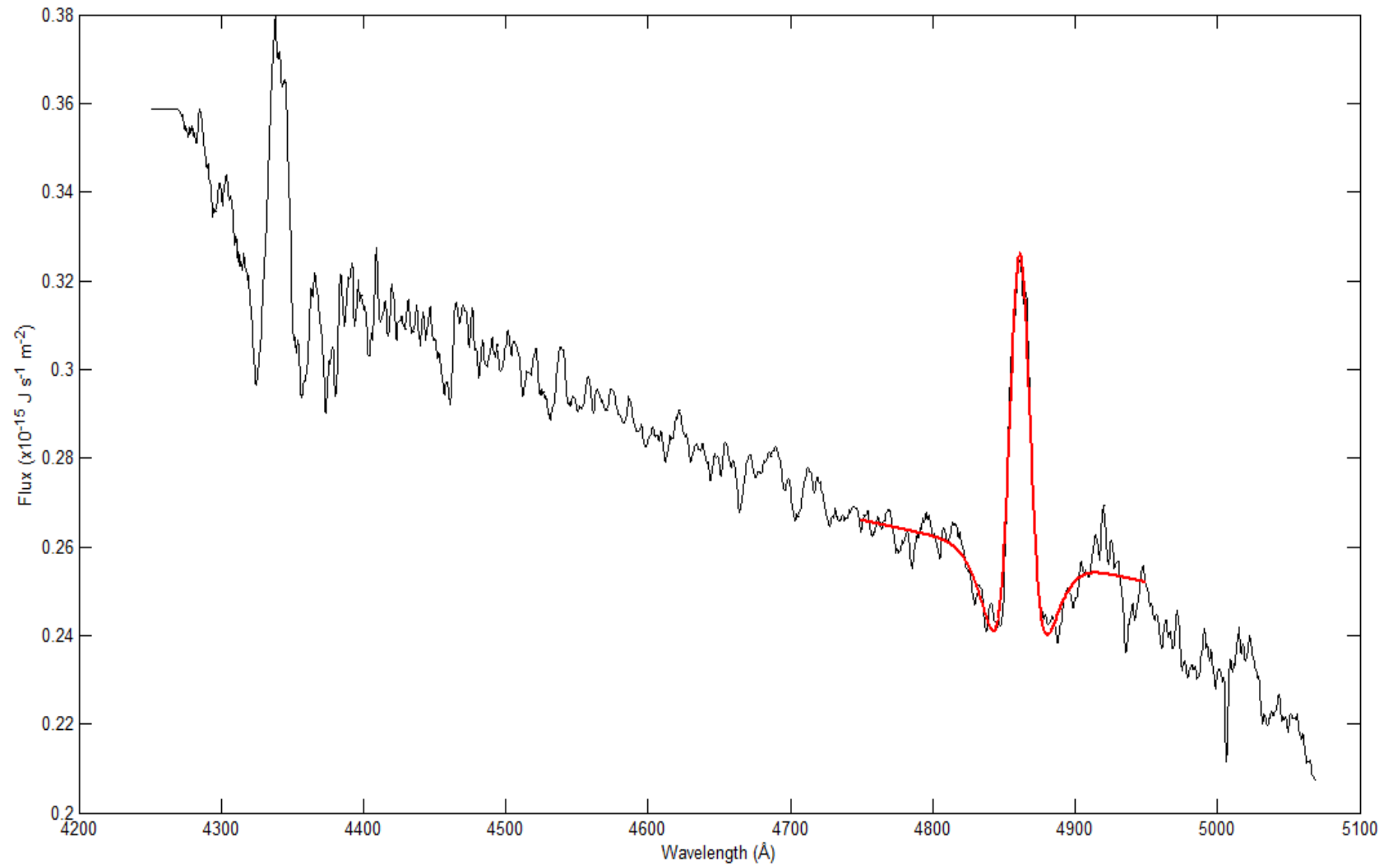


Figure 11: Spectrum and Gaussian fit for June 18, 1987.

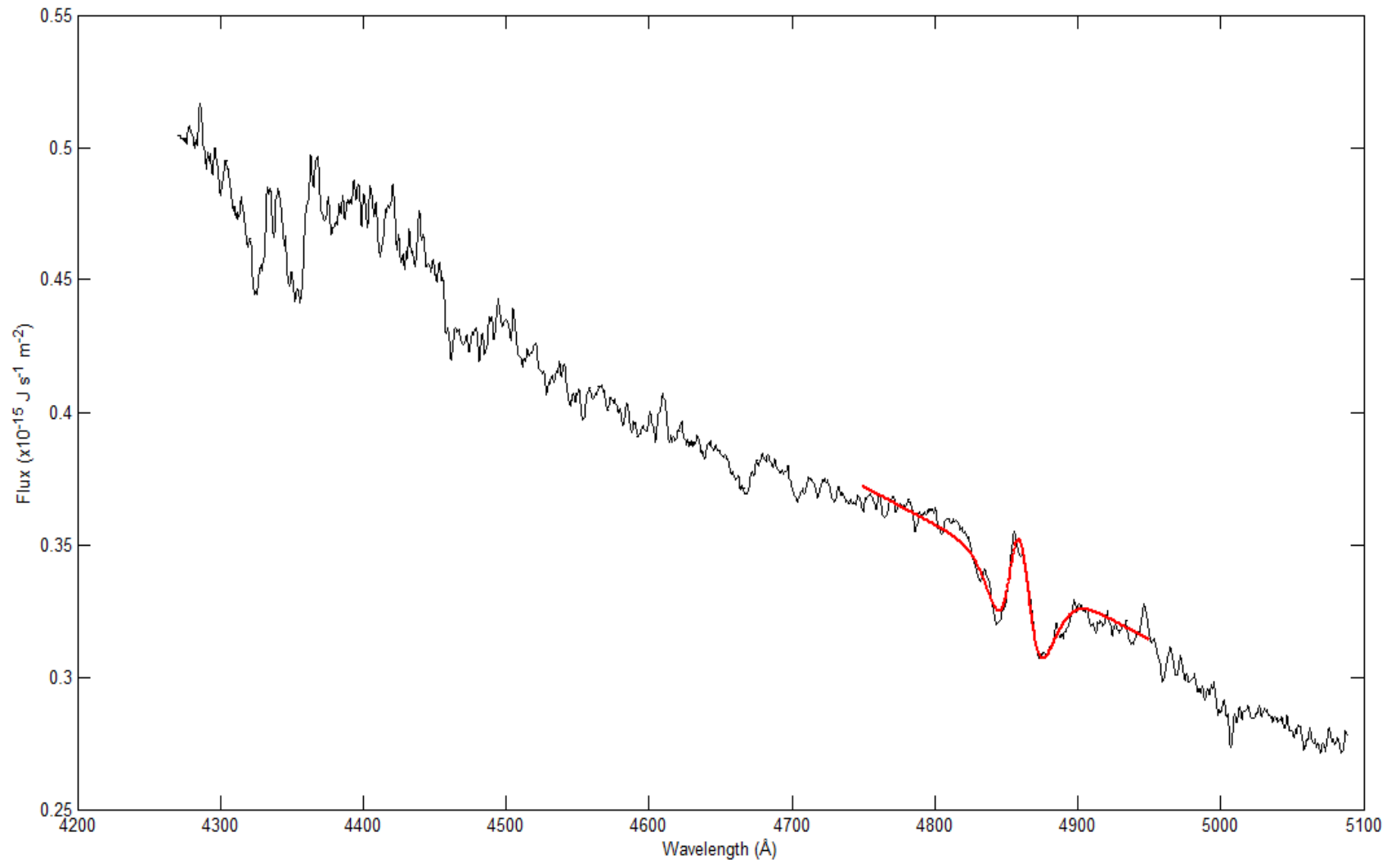


Figure 12: Spectrum and Gaussian fit for June 19, 1987.

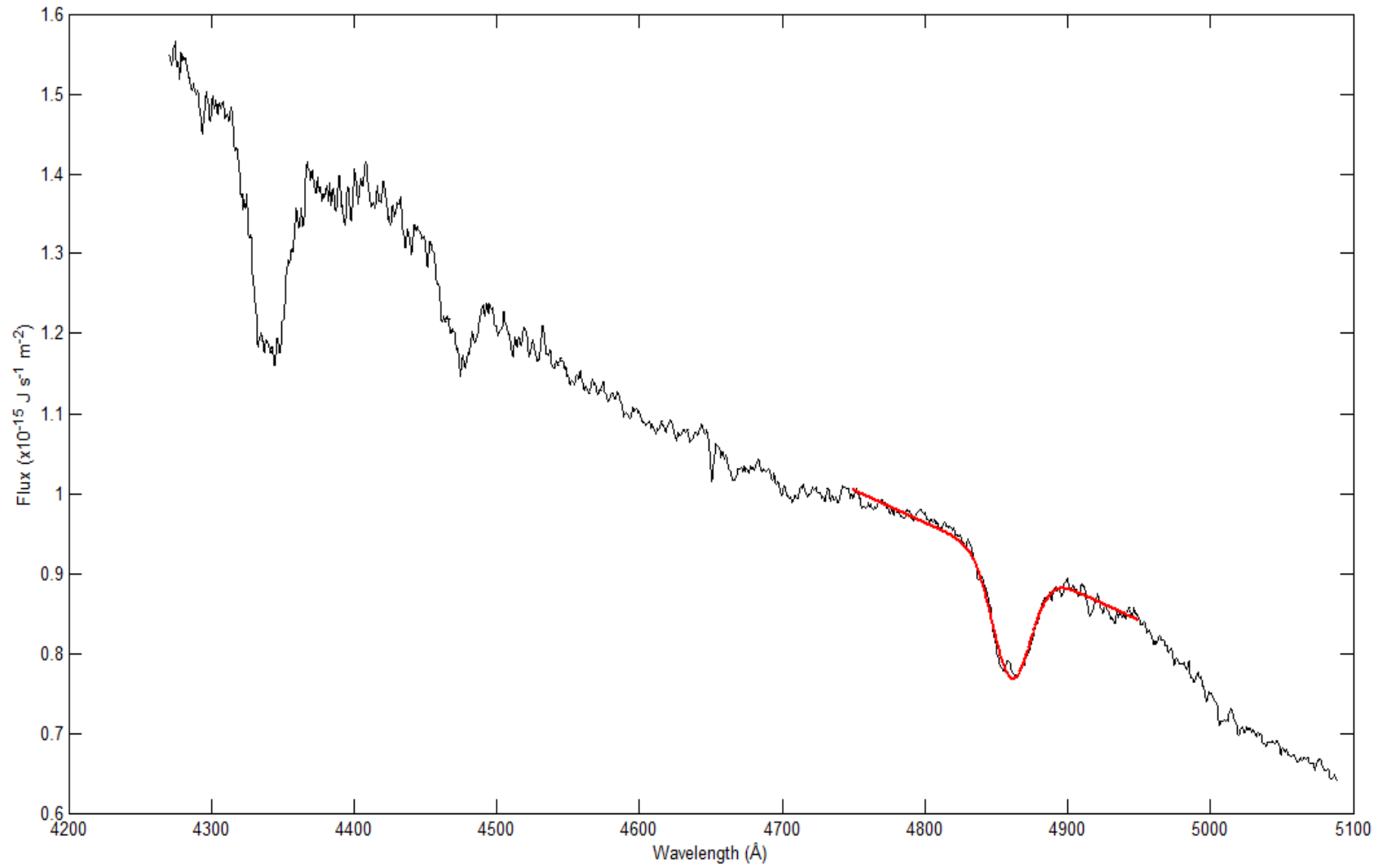


Figure 13: Spectrum and Gaussian fit for June 20, 1987.

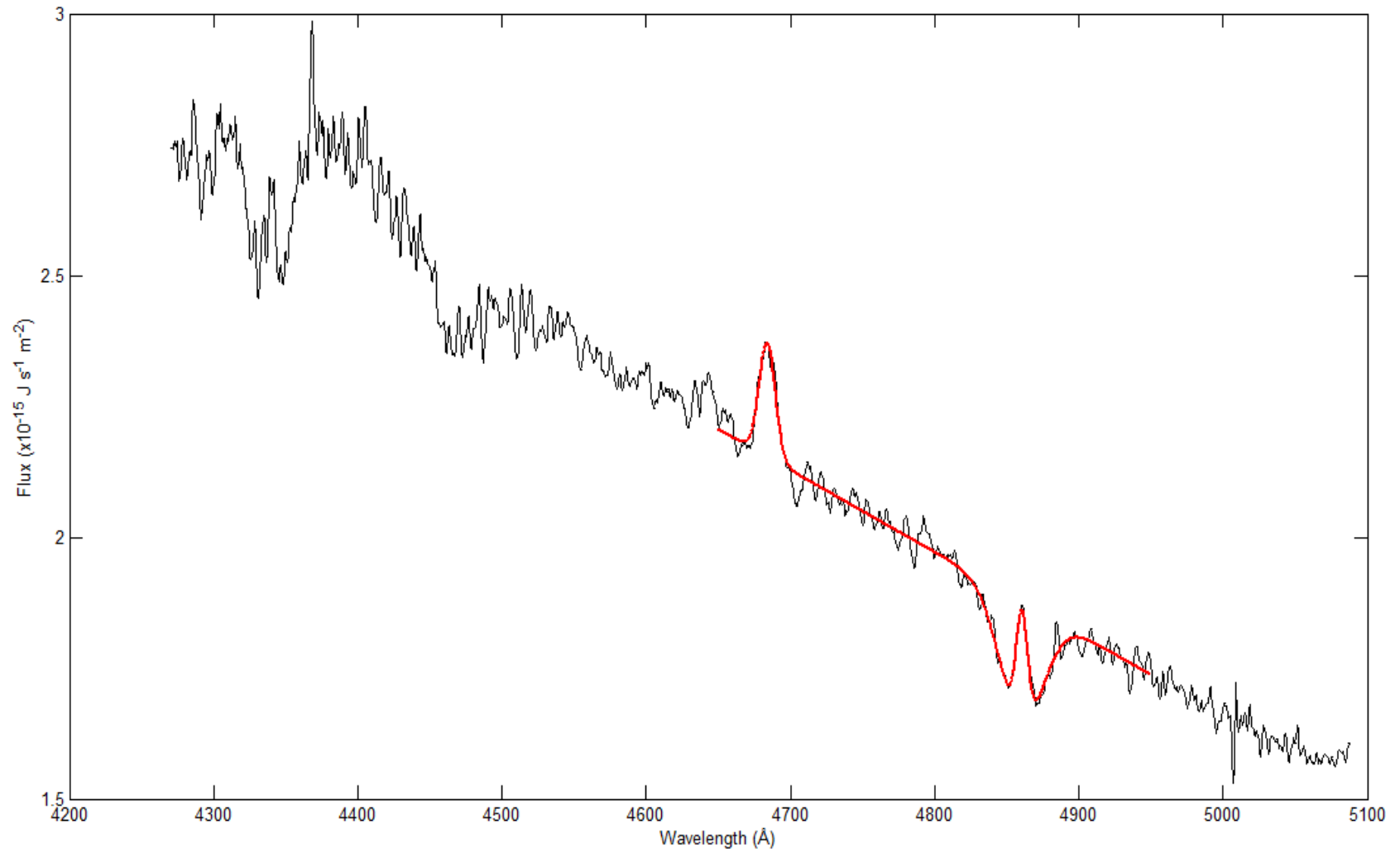


Figure 14: Spectrum and Gaussian fit for June 21, 1987.

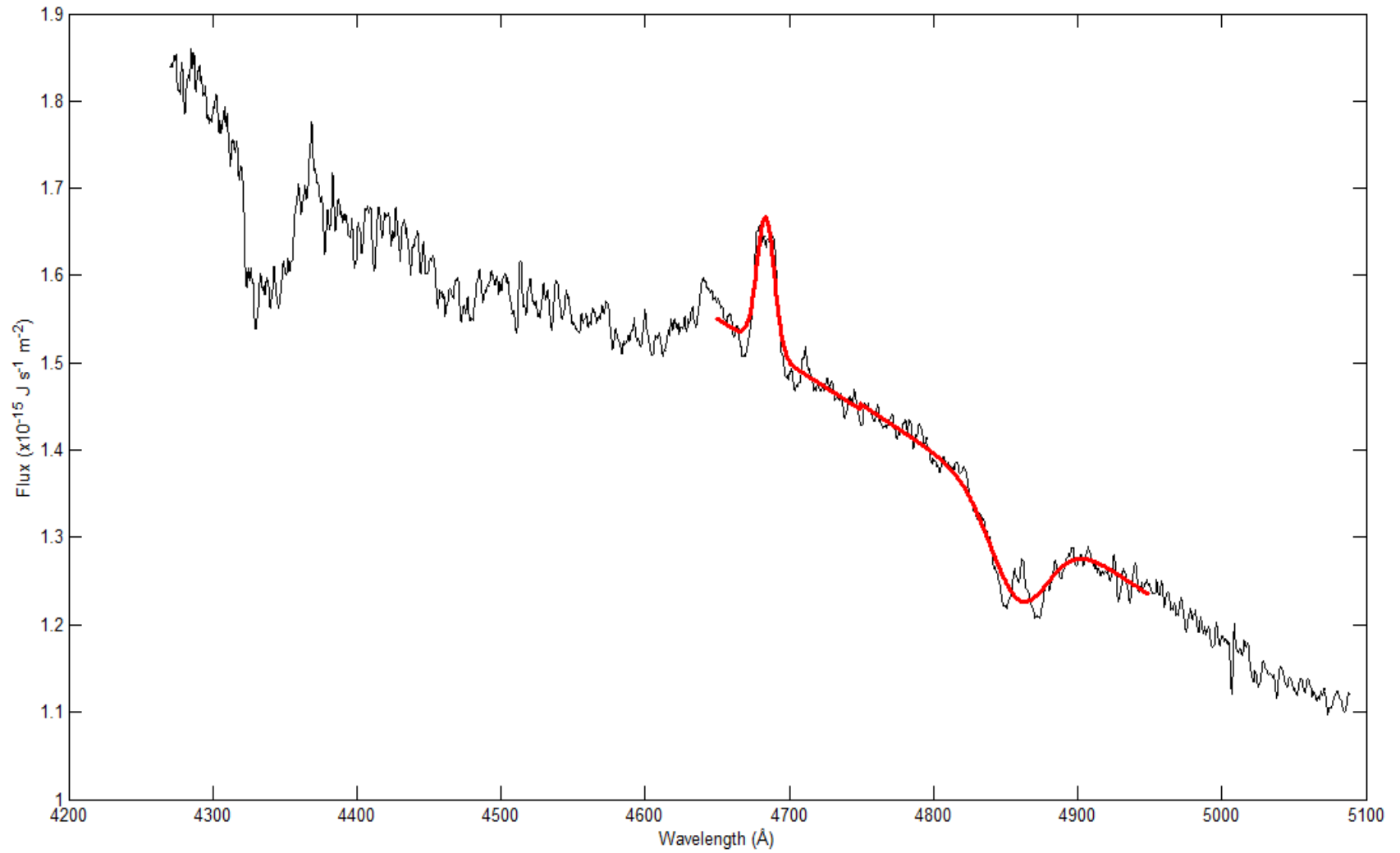


Figure 15: Spectrum and Gaussian fit for June 22, 1987.

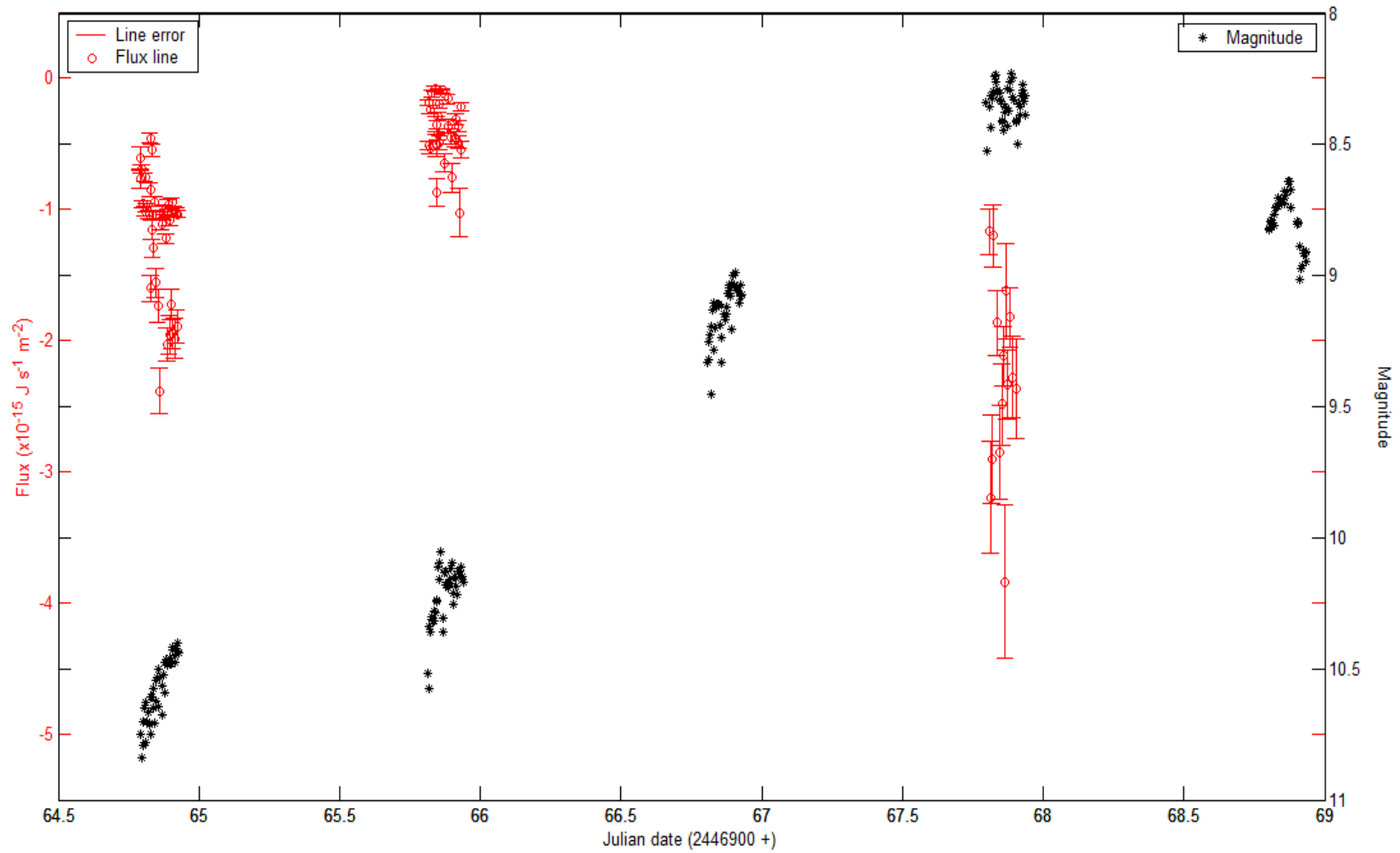


Figure 16: Flux of the $H\beta$ (4861Å) emission lines vs. Julian date through the outburst.

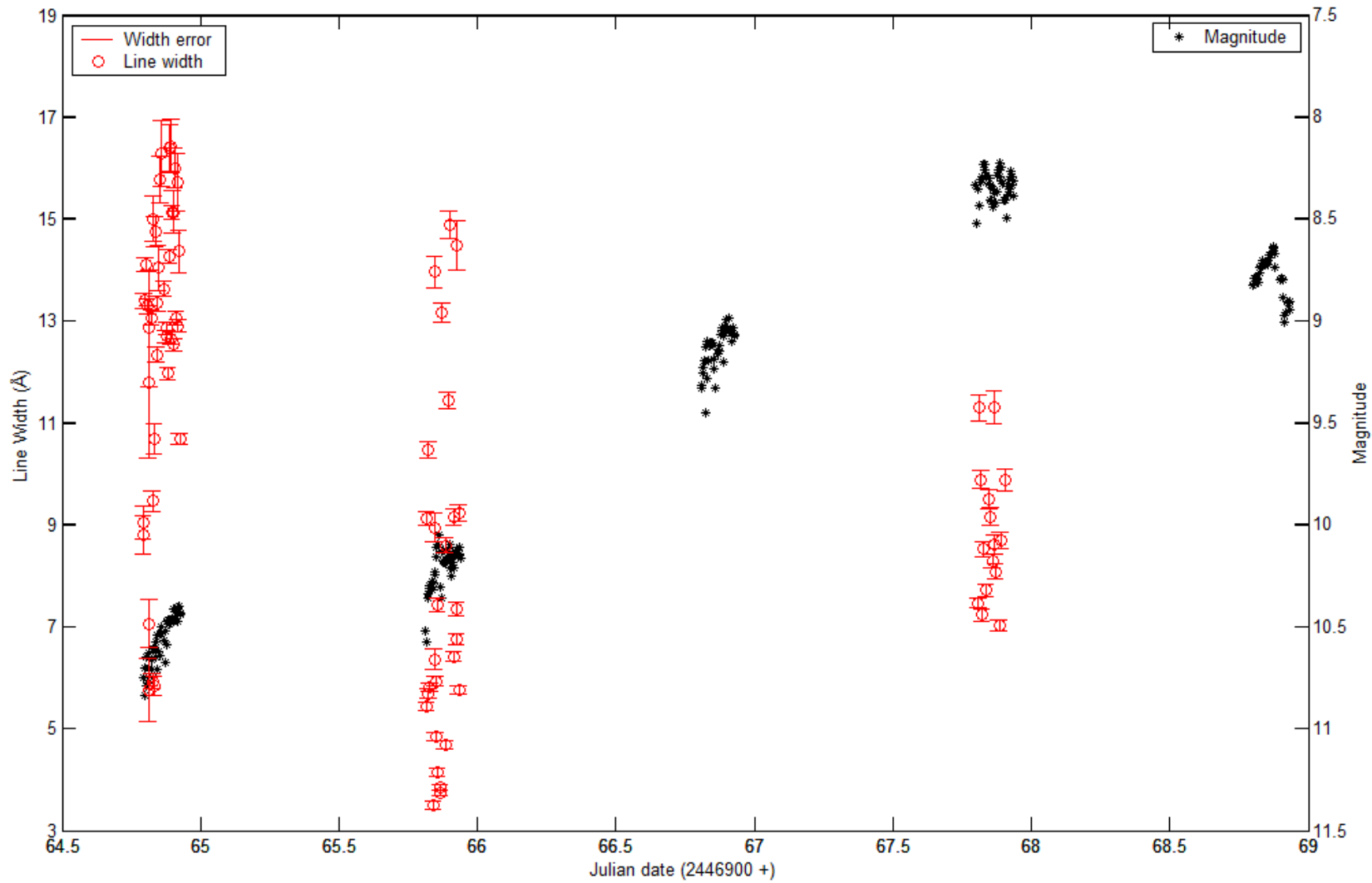


Figure 17: $H\beta$ (4861Å) emission line width vs. Julian date through the outburst.

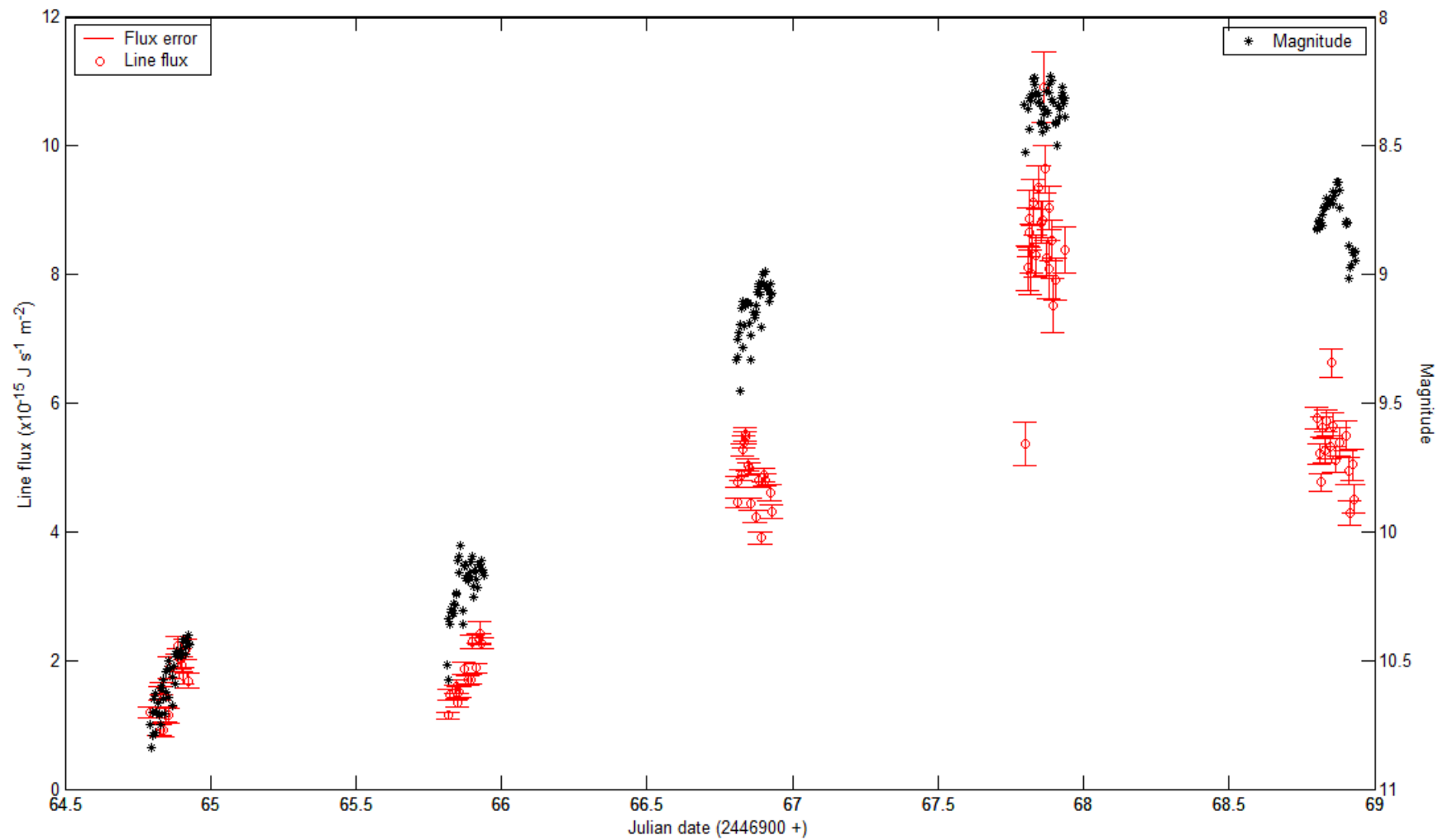


Figure 18: $H\beta$ (4861Å) absorption line Flux vs. Julian date through outburst.

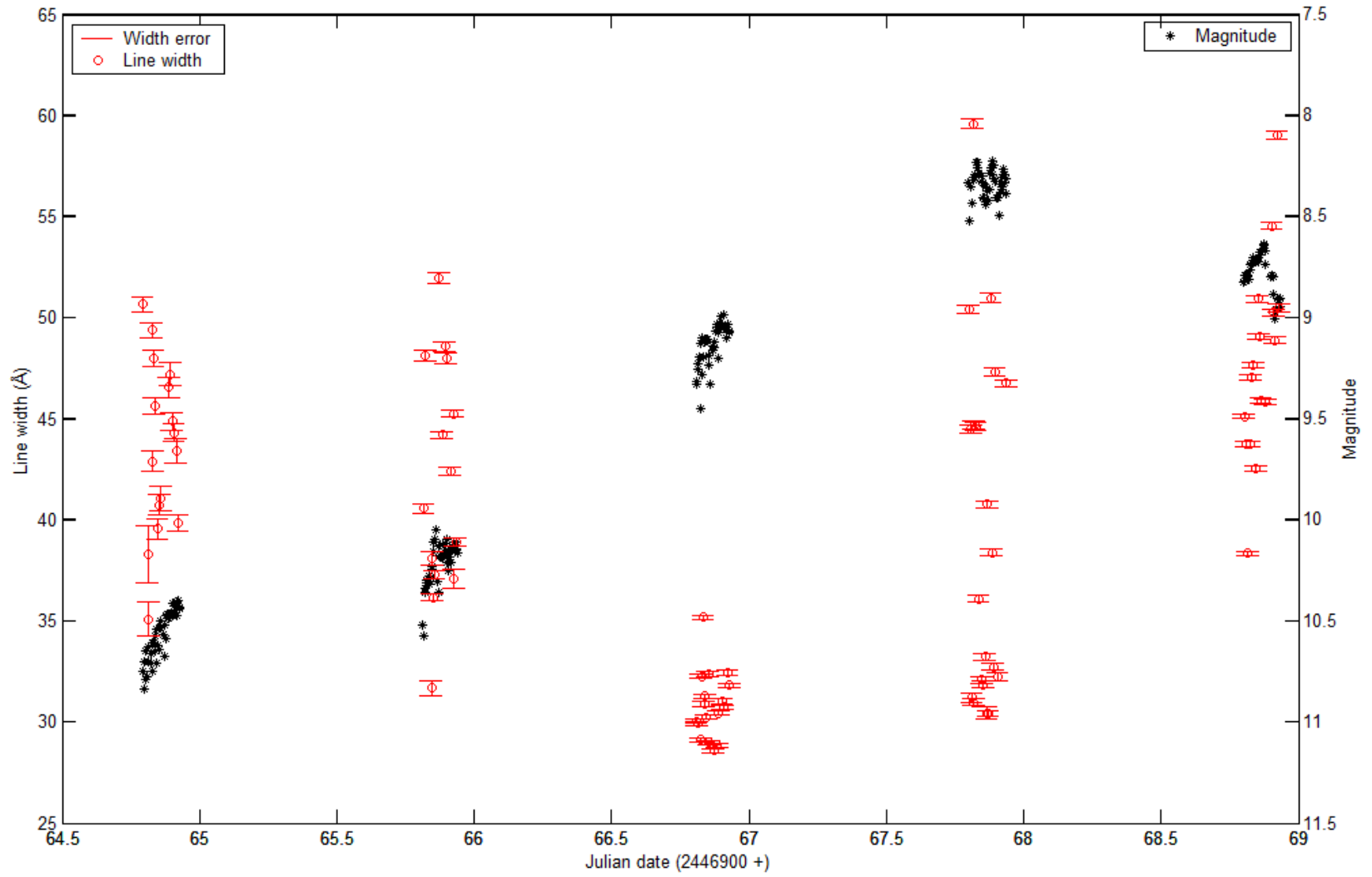


Figure 19: $H\beta$ (4861\AA) absorption line width vs. Julian date through outburst.

Figures 20, 21 and 22 show the flux and width of the HeII ($\lambda 4686$) emission lines throughout the outburst. It can be seen how the flux is spread between $-2 \times 10^{-15} \frac{J}{s m^2}$ and $-5 \times 10^{-15} \frac{J}{s m^2}$ for the first night HeII is detected and between $-2 \times 10^{-15} \frac{J}{s m^2}$ and $-3 \times 10^{-15} \frac{J}{s m^2}$ for the second night HeII is detected. It also shows how the width of the lines is between 10\AA and 15\AA on the 21st and between 12\AA and 17\AA on the 22nd.

On figure 21, the HeII ($\lambda 4686$) emission lines showed an increase on the first day the lines were detected and a relatively constant flux on the second day it was detected. The behavior of the HeII ($\lambda 4686$) emission lines would be a factor that can support the disk instability model. In this model the mass transfer from the main sequence star is constant while the accretion disk is unstable. When the instability reaches a critical amount, the outburst occurs. The rise in the flux of the HeII emission lines shows when the instability reaches its critical point and the energy is enough to produce these lines.

Using the central wavelength that was determined with the Gaussian fit program the Doppler shift of the lines was obtained which gave the radial velocity. A plot of the radial velocity of both H β ($\lambda 4861$) and HeII ($\lambda 4686$) can be seen in figures 23 and 24. Using a cosine fit program and a periodicity program an epoch, amplitude and period were found for the H β ($\lambda 4861$) radial velocity. The data has an amplitude of $52.98\text{km/s} \pm 12$, a maximum around 0.4 of the orbital phase and a minimum around 0.1 and 0.9 of the orbital phase. The orbital phase used in this study is a calculated one therefore the plots might be off phase compared to other studies. The orbital phase was calculated using a program that follows the tendencies of the data inputted and the orbital period of the system. These values can be different than other studies since these systems have

orbital variations making it close to impossible to determine an exact orbital phase that anyone can use.

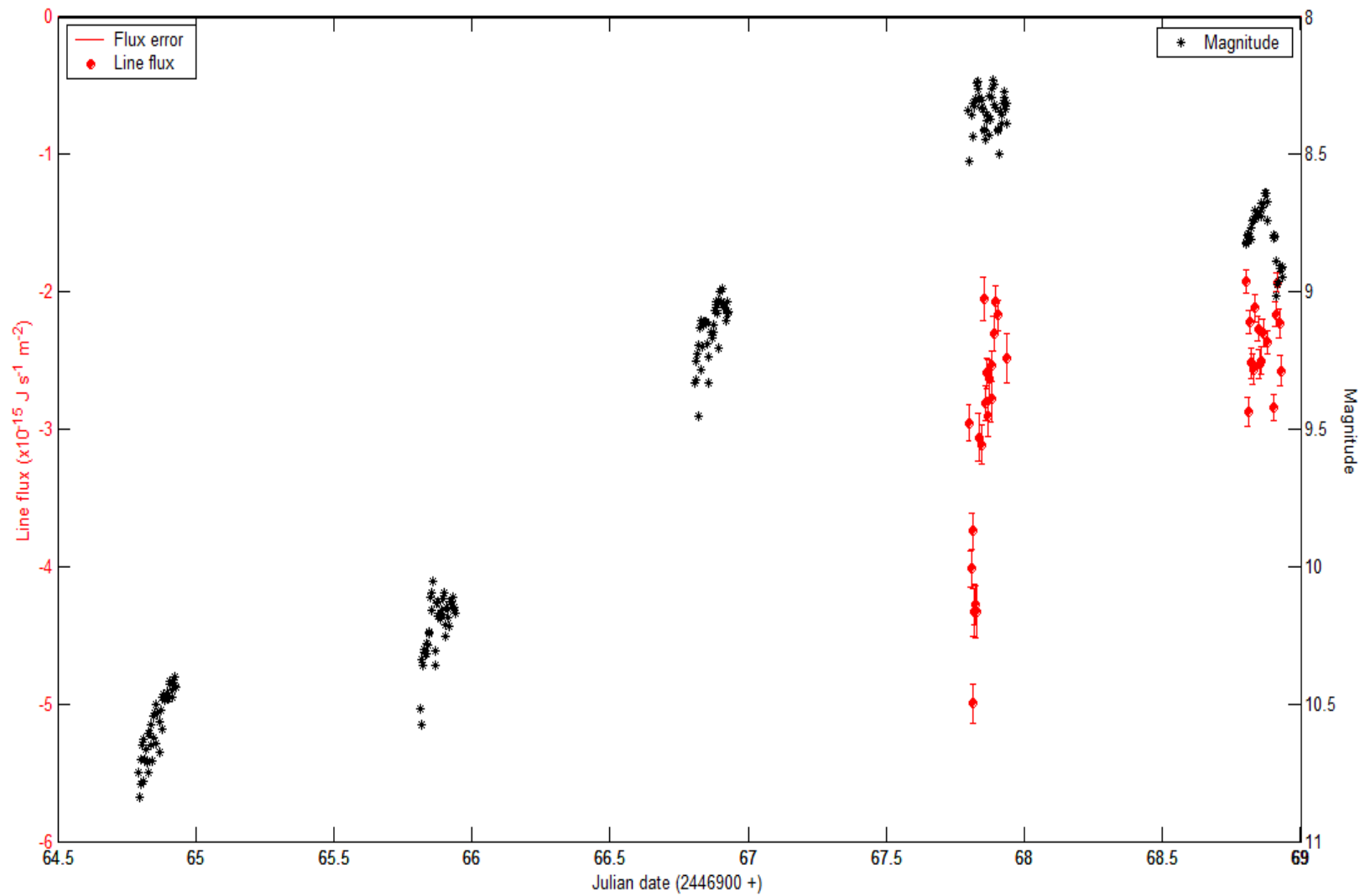


Figure 20: HeII (4686Å) emission line flux vs. Julian date through the outburst.

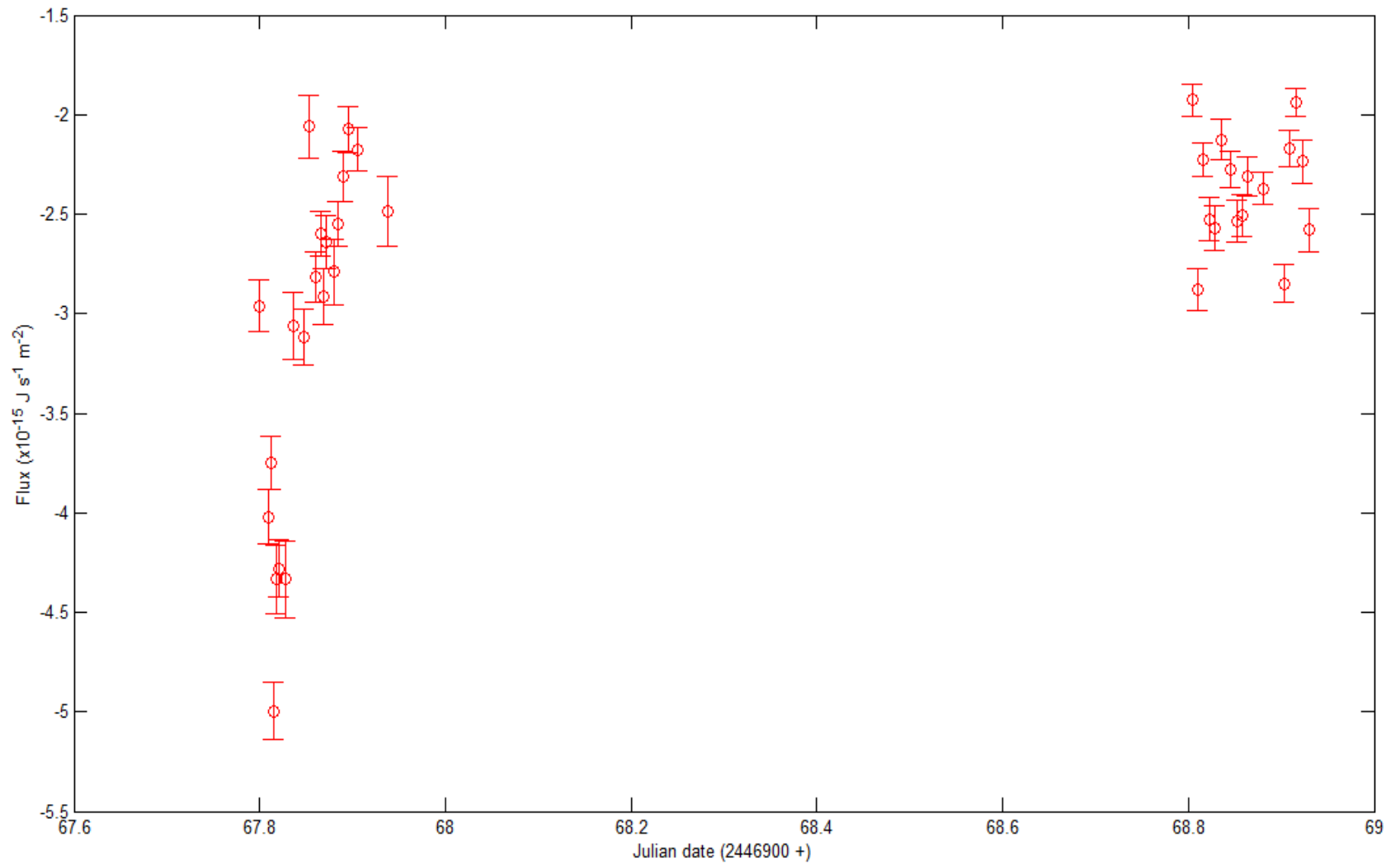


Figure 21: HeII (4686Å) emission line flux vs. Julian date

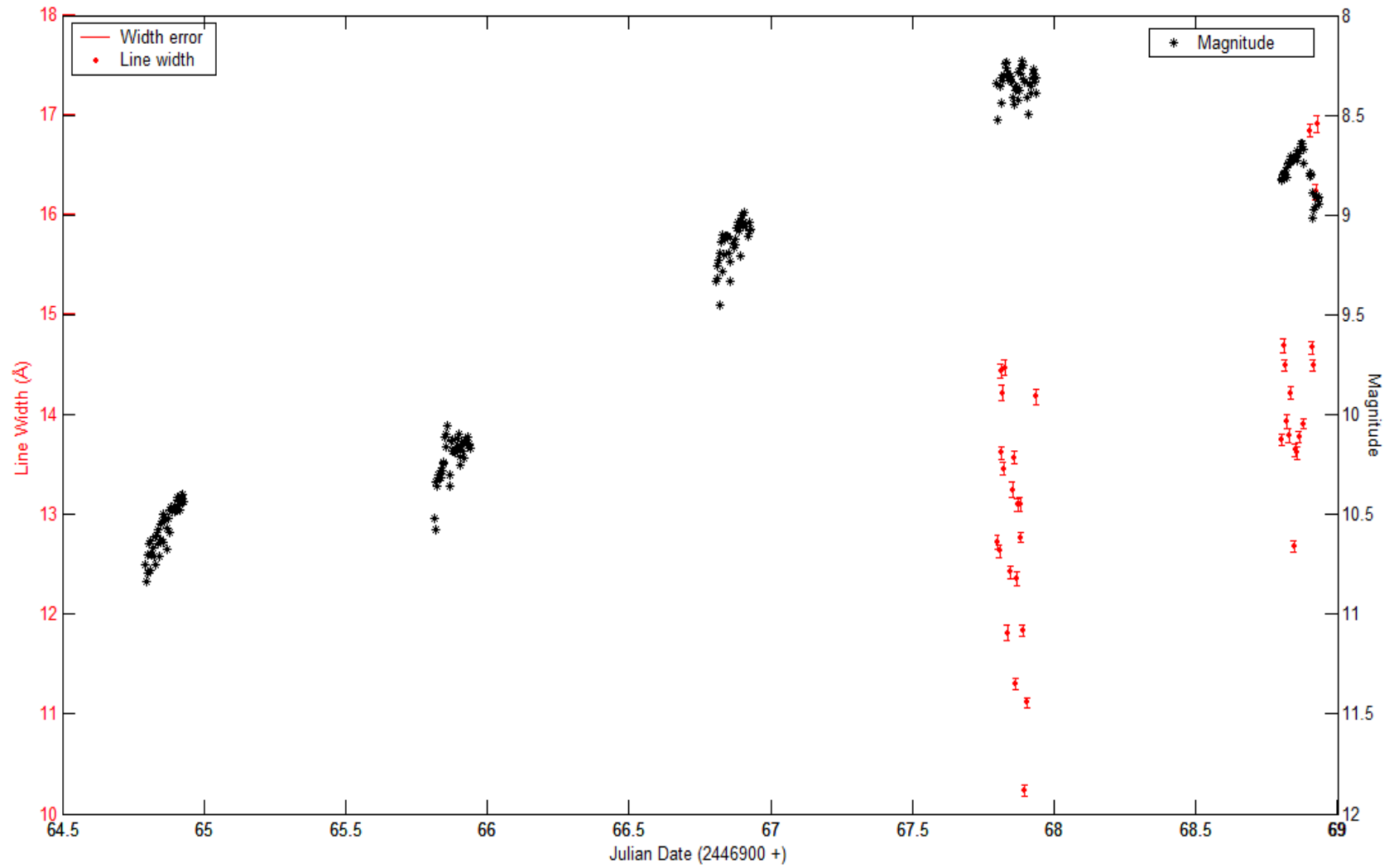


Figure 22: Widths of the HeII (4686Å) emission lines vs. Julian date through the outburst

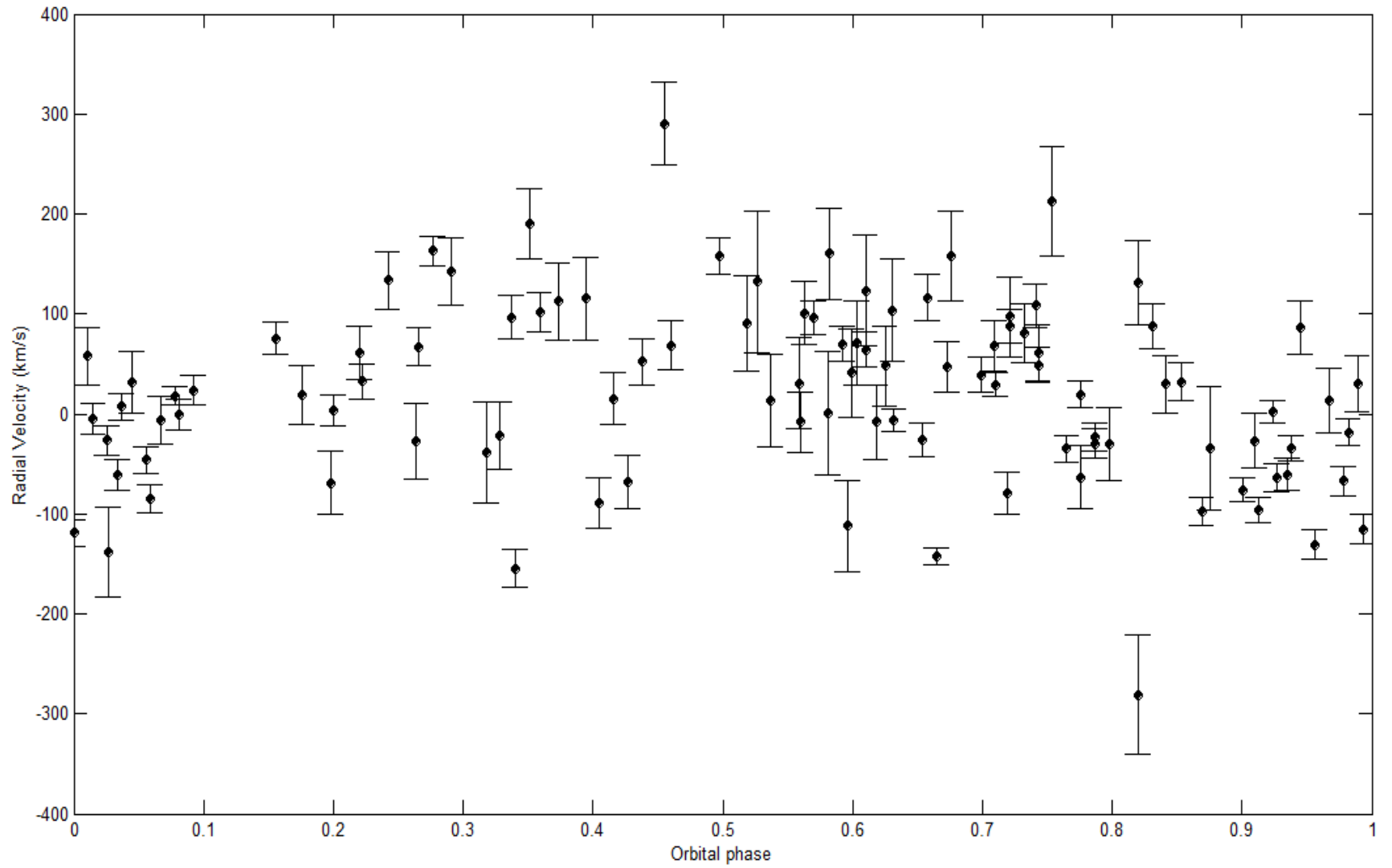


Figure 23: Radial velocity of H β ($\lambda 4861$) vs. orbital phase.

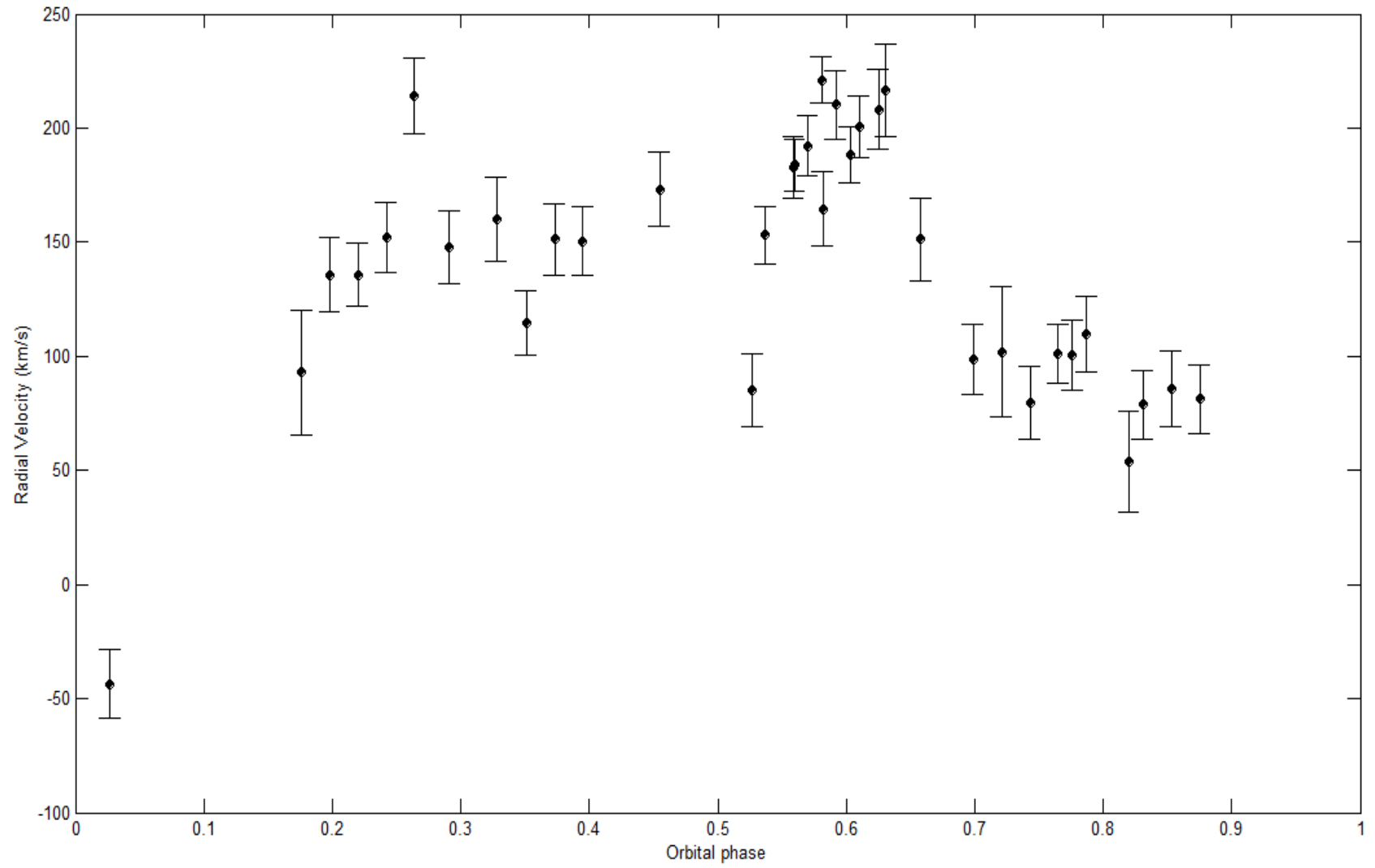


Figure 24: Radial velocity of HeII ($\lambda 4686$) vs. orbital phase

SUMMARY

The analysis of the spectra in this study has provided a look into the behavior of dwarf novae during outburst. The strength of the lines in some spectra was different than expected in some cases because during the outburst the emission lines can flicker and in others the weather was possibly a factor. The first night of the September 1985 observation was the day after some rain and thunderstorms had passed by. There is a possibility that there were clouds that would affect the observations for that night. For the night of June 22 a concern was trying to understand why the flux was lower than what was registered by the AAVSO and lower than the previous night. After looking for any notes and how the weather was that night there was no real explanation as to why this happened. Similar to the September 1985 weather, there were some rain and thunderstorms after this night which could mean that it is all due to clouds affecting the observations, but there is no concrete answer.

When comparing the AAVSO data to the magnitudes obtained from the spectra the same trend can be observed with a bit of a difference since the AAVSO data was observed in the visual range while the spectra in this study were detected in a mix between visual and blue. As the nights during outburst are compared, an increase in the strength of the H β (λ 4861) absorption lines and a decrease in the strength of the H β

($\lambda 4861$) emission lines as well as an increase in the strength of the HeII ($\lambda 4686$) emission lines mid outburst are seen.

A plot of the flux strength of the H β ($\lambda 4861$) emission lines showed an overall increase in the beginning of the outburst and a decrease mid outburst. This is also observed in the plot of the H β ($\lambda 4861$) emission lines width throughout the outburst. The H β ($\lambda 4861$) absorption line shows an increase in the flux while there is a decrease and then an increase of the widths of the lines.

A fit of the HeII ($\lambda 4686$) emission lines on the dates of June 21st and 22nd was also possible. The plots of the width and flux of the HeII ($\lambda 4686$) emission lines show an increase in these values mid-outburst. These observations as well as the observations regarding the H β ($\lambda 4861$) emission and absorption lines helped confirm the Instability model.

From all the data regarding the wavelength and flux of each emission and absorption lines a plot of the radial velocity was made. In it, it can be observed that the maximum radial velocity of the disk is approximately 200km/s. The radial velocity can be compared to the radial velocity calculated by Hessman (et al. 1981, 1986) which has a maximum velocity of 50km/s and a minimum of -100km/s for H β ($\lambda 4861$) and a maximum of 50km/s and a minimum of -200km/s for HeII ($\lambda 4686$). Hessman (et al. 1981) explains that the radial velocities were derived by cross-correlating the minimum light SS Cyg spectra with HD 213947, a K4 III star. The data used by Hessman (et al. 1981) consisted of spectra obtained in August and October 1981. The August data were obtained when the system was at minimum light and the October data were obtained mid-outburst through the end of the outburst.

In his study, Hessman associates the behavior of the emission lines to the phasing of the system and an increase in the mass transfer from the main sequence star. He also associates the HeII ($\lambda 4686$) emission lines to the existence of a really hot and luminous “hot spot” produced by the stream impact.

The behavior of the HeII ($\lambda 4686$) emission lines follows the disk instability model. As the material from the main sequence star is accreted, the disk becomes unstable until the instability is too high for the system. To stabilize the system the mass in the outer bounds of the accretion disk, where the emission lines are from, flows all at once to the center of the disk, where the absorption lines come from. This accretion makes the absorption lines wider and it is such a high energy process that it produces HeII ($\lambda 4686$) emission lines. The strength of the HeII ($\lambda 4686$) lines detected in this study increases at mid-outburst showing that the disk instability is the main reason for the outbursts.

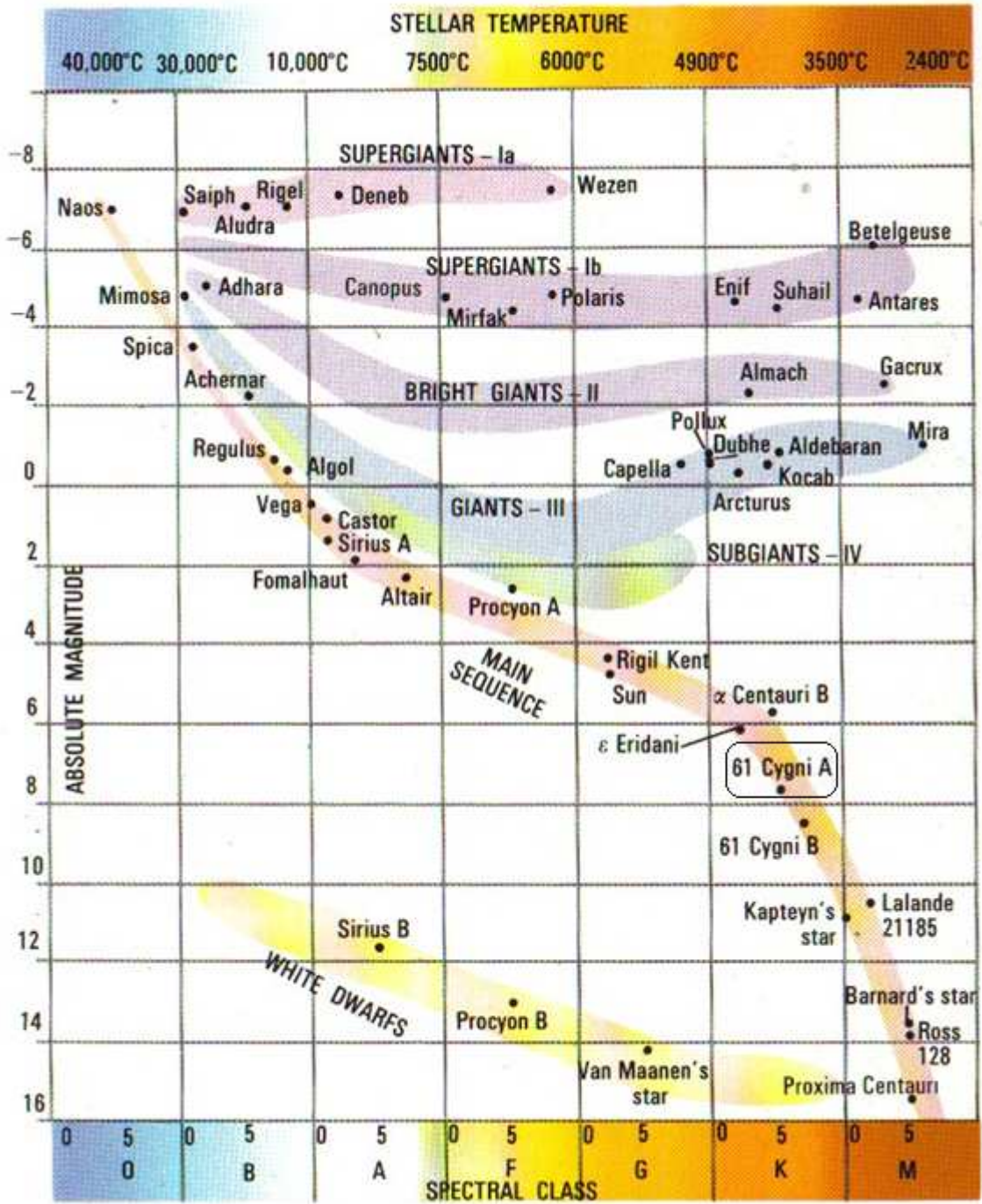
Since the data used on this study were from the beginning to mid-outburst it was possible to determine that the disk instability model was the best model for the behavior of dwarf novae. Hessman (et al. 1981) uses data obtained in a minimum and from mid-outburst to the end of the outburst, therefore they were not able to observe the behavior of the system as it rises into outburst.

The similarities between the results from this study and previous ones are satisfying. This study could progress further with the comparison of these spectra with newer spectra. This would help explain why Dwarf Novae behave the way they do and, with any luck, properly answer where does the outburst comes from.

APPENDIX

Appendix A: Figure 25: Hertzsprung-Russell diagram.

(<http://bdaugherty.tripod.com/gcseAstronomy/stars.html>)



Appendix B: Example of Output of the Gaussian fit program

FILE: z622 OBJECT: SS CYG DATE: 22-JUN-87
PROGRAM: NGAUSS

WAVELENGTH RANGE: 4750. 4950.
CENTRAL WAVELENGTHS: 4861.0
WIDTHS: 41.200
DEPTHS: .150
SLOPE: .000E+00
INTERCEPT: .161E-11
EXCLUDED INTERVALS:
MEAN ERROR PER POINT: .0000E+00
NUMBER OF POINTS IN FIT INTERVAL = 501

...
INTEGRATED LINE FLUX: LINE # 1 = .5299E-11
+++++
LINE 1:
DEPTH(INT) FWHM(ANG) POS(ANG) EW(ANG)
 TREND(INT/ANG) INTERCEPT
.0785 47.523 4859.45 3.97 -.10871E-03 .13335E-11
+++++
1

CHI-SQUARED PER DEGREE OF FREEDOM = .71400E-04
APPROX. MEAN STAND. DEV. PER POINT = .84498E-02

FILE: z622 OBJECT: SS CYG DATE: 22-JUN-87
PROGRAM: NGAUSS

WAVELENGTH RANGE: 4750. 4950.
CENTRAL WAVELENGTHS: 4861.0
WIDTHS: 41.200
DEPTHS: .150
SLOPE: .000E+00
INTERCEPT: .161E-11
EXCLUDED INTERVALS:
MEAN ERROR PER POINT: .8450E-02
NUMBER OF POINTS IN FIT INTERVAL = 501

...
INTEGRATED LINE FLUX: LINE # 1 = .5299E-11
+++++
LINE 1:

DEPTH(INT)	FWHM(ANG)	POS(ANG)	EW(ANG)
.0785	47.534	4859.46	.13335E-11
TREND(INT/ANG) INTERCEPT			
		3.97	-.10871E-03

+++++

1

CHI-SQUARED PER DEGREE OF FREEDOM = .10000E+01
APPROX. MEAN STAND. DEV. PER POINT = .10000E+01

*****ERRORS FROM STEPIT*****

ERRORS LINE 1:

DEPTH: .24865E-02
FWHM: .99258E+00
WAVELENGTH: .41185E+00
INTEGRATED FLUX: .12613E-12
EQUIVALENT WIDTH: .94630E-01

SLOPE: .69629E-05
INTERCEPT: .95592E-15

...

*****ERRORS FROM FIDO*****
(PPLUS)

ERRORS LINE 1:

DEPTH: .24865E-02
FWHM: .99258E+00
WAVELENGTH: .41184E+00
INTEGRATED FLUX: .12613E-12
EQUIVALENT WIDTH: .94630E-01

SLOPE: .69629E-05
INTERCEPT: .95589E-15

(MINUS)

ERRORS LINE 1:

DEPTH: -.24865E-02
FWHM: -.99258E+00
WAVELENGTH: -.41184E+00
INTEGRATED FLUX: -.12613E-12
EQUIVALENT WIDTH: -.94630E-01

SLOPE: -.69629E-05
INTERCEPT: -.95589E-15

LITERATURE CITED

1. Adams W.S. and Joy A.H.. Spectroscopic notes on some variable stars. In Twenty-Seventh Meeting of the American Astronomical Society. Popular Astronomy (1921), 102--103.
2. American Association of Variable Star Observers. AAVSO: Light Curve Generator. <http://aavso.org/data/lcg/>
3. Bonnarel F., Fernique P., Bienayme O., Egret D., Genova F., Louys M., Ochsenbein F., Wenger M. and Bartlett J.G.. The ALADIN interactive sky atlas. A reference tool for identification of astronomical sources. Astronomy and Astrophysics Supplement Series (2000), no. 143, 33-40.
4. Byard P.L., Foltz C.B., Jenkner H. and Peterson B.M.. The Ohio State image Dissector Scanner. Publications of the Astronomical Society of the Pacific (1981), no. 93, 147--153.
5. Carroll B.W. and Ostlie D.A.. An Introduction to Modern Galactic Astrophysics and Cosmology. 2nd ed, A. Black and A.T. Anderson, Pearson Education, San Francisco, CA (2007).
6. Claudi R.. Tesi di laurea in Fisica. Università 'La Sapienza' of Roma, Italy (1986).
7. Cannon Smith R.. Cataclysmic Variables. astro-ph/0701654

8. Copeland E., 1882, *Observatory*, **5**, 100
9. Crawford J.A. and Kraft R.P.. An Interpretation of AE Aquarii. *Astrophysical Journal* (1956), no. 123, 44--53.
10. Elvey C.T. and Babcock H.W.. The spectra of U Geminorum type variable stars. *Astrophysical Journal* (1943), no. 97, 412--426.
11. Fleming W.P.S.. Stars having peculiar spectra. *Annals of the Astronomical Observatory of Harvard College* (1912), no. 56, 165--226.
12. Hessman, F.V., Robinson, E.L., Nather, R.E. and Zhang, E.H.. Time-resolved spectroscopy of SS Cygni at minimum and maximum light. *Astrophysical Journal* (1984), no 286, 747-759.
13. Hessman F.V., The spectrum of SS Cygni during a dwarf novae eruption. *Astrophysical Journal* (1986), no. 300, 794--803.
14. Hind J.R.. On a new variable star. *Monthly Notices of the Royal Astronomical Society* (1856), no. 16, 56.
15. Hinderer F.. Spektralphotometrische Untersuchungen über den Veränderlichen Ss Cygni. *Astronomische Nachrichten* (1949), no. 277, 193--222.
16. Joy A.H.. Spectroscopic Observations of SS Cygni variables. *Publications of the Astronomical Society of the Pacific* (1940), no. 52, 324--325.
17. Joy A.H.. Radial-Velocity measures of SS Cygni at maximum light. *Astrophysical Journal* (1956), no. 124, 317--320.
18. Knott G.. The variable U Geminorum. *The Observatory* (1882), no. 5, 110--111.
19. Kraft R.P.. Binary Stars among Cataclysmic Variables. I. U Geminorum Stars (dwarf Novae). *Astrophysical Journal* (1962), no. 135, 408--423.

20. Kraft R.P., 1964, in First Conference on Faint Blue Stars, ed W.J. Luyten, Univ. Minn. Press, Minneapolis, 77
21. Paczynski B.. Evolutionary Processes in Close Binary Systems. Annual Review of Astronomy and Astrophysics (1971), no. 9, 183--208.
22. Patterson J.. The evolution of cataclysmic and low-mass X-ray binaries. Astrophysical Journal Supplement Series (1984), no. 54, 443--493.
23. Peters C.H.F.. Über zwei neue Veränderliche. Astronomische Nachrichten (1865), no. 65, 55--60.
24. Peterson B.M.. IRS User's Manual (1988), Department of Astronomy, Ohio State University (Internal Rep. Ser., No. 88-001)
25. Pickering E.C. and Fleming W.P.. Harvard College Observatory, circular no. 12. Stars having peculiar spectra. New variable stars in Crux and Cygnus. Astrophysical Journal (1896), no. 4, 369
26. Pogson N.. On the variable star U Geminorum. Monthly Notices of the Royal Astronomical Society (1857), no. 17, 200--202.
27. Pringle J.E.. Accretion disks in Astrophysics. Annual Review of Astronomy and Astrophysics (1981), no. 19, 137--162.
28. Samus N.N. and Durlevich O.V.. Combined general catalogue of variable stars. VizieR On-line data catalogue (2004).
29. Smak J.. On the rotational velocities of gaseous rings in close binary systems. Acta Astronomica (1969), no. 19, 155--164.
30. Smak J.. Accretion in cataclysmic binaries. IV – Accretions disks in dwarf novae. Acta Astronomica (1984), no. 34, 161--189.

31. Smak J.. Accretion disks in Algols. *Space Science Reviews* (1989), no. 50, 107--116.
32. Smak J.. Cataclysmic variables. In: F.C. Lázaro and M.J. Arévalo editors. *Binary Stars: Selected Topics on Observations and Physical Processes*. Springer Publisher, Tenerife, Spain (2001), 110--150.
33. Van Biesbroek D.. *Annales de l'Observatoire Royal de Belgique* (1904), no. 13, 21.
34. Verbunt F.. Accretion disks in stellar X-ray sources - A review of the basic theory of accretion disks and its problems. *Space Science Reviews* (1982), no. 32, 379--404.
35. Wachmann A.A.. Photographische Beobachtungen von Veränderlichen auf dem Kapteyn-Eichfeld 41. *Astronomische Nachrichten* (1935), no. 255, 341--380.
36. Walker M.F.. Nova DQ Herculis (1934): an Eclipsing Binary with Very Short Period. *Publications of the Astronomical Society of the Pacific* (1954), no. 66, 230--232.
37. Warner B.. Absolute magnitudes of cataclysmic variables. *Monthly Notices of the Royal Astronomical Society* (1987), no. 227, 23--73.
38. Warner B.. *Cataclysmic Variable Stars*. A. King and D. Lin, Cambridge University Press, Cambridge, MA (1995).
39. Webbink R.F.. *The Astronomy and Astrophysics Encyclopedia*. S.P. Maran, Cambridge University Press, Cambridge, MA (1991).
40. Weather Underground, <http://www.wunderground.com/history/>